Atmospheric
Measurement
Techniques
Discussions

1 # UAS Chromatograph for Atmospheric Trace Species
2 # (UCATS) – a versatile instrument for trace gas
3 # measurements on airborne platforms
4
5 Eric J. Hintsa,[1,2] Fred L. Moore,[1,2] Dale F. Hurst,[1,2] Geoff S. Dutton,[1,2] Bradley D. Hall,[2] J. David
6 Nance,[1,2] Ben R. Miller,[1,2] Stephen A. Montzka,[2] Laura P. Wolton,[1,2] Audra McClure-Begley,[1,2]
7 James W. Elkins,[2] Emrys G. Hall,[1,2] Allen F. Jordan,[1,2] Andrew W. Rollins,[3] Troy D.
8 Thornberry,[1,3] Laurel A. Watts,[1,3] Chelsea R. Thompson[1,3], Jeff Peischl[1,3], Ilann Bourgeois[1,3],
9 Thomas B. Ryerson,[3] Bruce C. Daube,[4] Jasna V. Pittman,[4] Steven C. Wofsy,[4] Eric Kort,[5] Glenn
10 S. Diskin,[6] and T. Paul Bui[7]
11
12 [1]Cooperative Institute for Research in Environmental Sciences, University of Colorado, Boulder, 80309, U.S.A.
13 [2]Global Monitoring Laboratory, NOAA, Boulder, CO 80305, U.S.A.
14 [3]Chemical Sciences Laboratory, NOAA, Boulder, CO 80305, U.S.A.
15 [4]Department of Earth and Planetary Sciences, Harvard University, Cambridge, MA 02138, U.S.A.
16 [5]Climate and Space Sciences and Engineering, University of Michigan, Ann Arbor, MI 48109
17 [6]NASA Langley Research Center, Hampton, VA 23681, U.S.A.
18 [7]NASA Ames Research Center, Mountain View, CA 94035, U.S.A.
19
20 *Correspondence to*: Eric Hintsa (Eric.J.Hintsa@noaa.gov)

Atmospheric
Measurement
Techniques
Discussions

1   **Abstract.** UCATS (the UAS Chromatograph for Atmospheric Trace Species) was designed and built for
2   observations of important atmospheric trace gases from unmanned aircraft systems (UAS) in the upper
3   troposphere and lower stratosphere (UT/LS). Initially it measured major chlorofluorocarbons (CFCs) and the
4   stratospheric transport tracers nitrous oxide (N_2O) and sulfur hexafluoride (SF_6), using gas chromatography
5   with electron capture detection. Compact ozone (O_3) and water vapor (H_2O) instruments were added to
6   enhance science missions on platforms with relatively small payloads. Over the past decade, UCATS has been
7   reconfigured to measure methane (CH_4), carbon monoxide (CO), and molecular hydrogen (H_2) instead of CFCs
8   and has undergone numerous upgrades to its subsystems. It has served as part of large payloads on
9   stratospheric UAS missions to probe the tropical tropopause region and transport of air into the stratosphere,
10   in piloted aircraft studies of greenhouse gases, transport, and chemistry in the troposphere, and will soon
11   return to the study of stratospheric ozone depletion, one of the original goals for UCATS. Each deployment
12   brought different challenges, which were largely met or resolved. The design, capabilities, modifications and
13   some results from UCATS are shown and described here, including changes for upcoming missions.
14
15   **1 Introduction**
16
17   Accurate and precise measurements of trace gases and other atmospheric parameters have resulted in an
18   ever more detailed understanding of the chemistry and physics of Earth's atmosphere. This has allowed
19   progress on environmental issues of global concern, including stratospheric ozone depletion and air pollution
20   in the lower atmosphere. For example, after the first report of the Antarctic "ozone hole" [Farman et al.,
21   1985], a combination of measurements from balloons, aircraft, and satellites, backed by a wide range of
22   laboratory, theoretical and modeling studies, allowed a sufficient grasp of the problem to relatively quickly
23   develop an effective international response [Douglass et al., 2014]. Though ozone loss and organic halogen
24   emissions are still ongoing matters of concern, climate change driven by greenhouse gas emissions is now the
25   overarching environmental problem today, while air quality continues to be an important issue as well.
26
27   The Halocarbons and other Atmospheric Trace Species (HATS) group in the Global Monitoring Laboratory
28   (GML, formerly Global Monitoring Division, GMD) at the National Oceanic and Atmospheric Administration
29   (NOAA) in Boulder, CO has long been involved in measuring N_2O, CFCs and other trace gases, primarily by
30   using gas chromatography with electron capture detectors (ECDs). This led to participation in a series of
31   airborne missions to study halogen budgets, ozone loss, and stratospheric transport, starting on the NASA ER-
32   2 aircraft in 1991 (Elkins et al., 1996). With the advent of unmanned aircraft systems (UAS), the potential
33   emerged to extend scientific airborne missions to higher altitudes, longer durations, and other experiments
34   that were not possible with manned aircraft. In addition, UAS could eliminate some of the danger of flying
35   piloted aircraft in remote regions. Accordingly, the UAS Chromatograph for Atmospheric Trace Species
36   (UCATS) was designed and built to measure ozone-depleting substances (ODS) and other trace gases on UAS
37   missions. These began in 2005 with the NOAA UAS Demonstration Mission [Fahey et al., 2006] on the Altair
38   aircraft, a high altitude version of the General Atomics Predator B adapted for use by NASA. Given the limited
39   payload capacity of Altair, small and lightweight ozone and water vapor sensors were installed inside UCATS
40   to generate a data set that could be interpreted without relying on other instruments. After two missions on
41   Altair, UCATS joined the payload of the National Science Foundation/National Center for Atmospheric
42   Research (NSF/NCAR) Gulfstream-V (GV) for the START-08 (Stratosphere-Troposphere Analyses of Regional
43   Transport; 2008) and HIPPO (HIAPER Pole-to-Pole Observations; 2009-11) missions [Pan et al., 2010; Wofsy,
44   2011]. These large-scale, piloted missions included vertical profile measurements from 150 m above the sea
45   surface up to the lower stratosphere. In 2010, UCATS returned to its original purpose, flying on the NASA
46   Global Hawk UAS for the Global Hawk Pacific (GloPac) science demonstration project. From 2011 to 2014,
47   UCATS participated in the Airborne Tropical Tropopause Experiment (ATTREX; Jensen et al., 2013), also on
48   the Global Hawk, to study dehydration, transport, and ozone chemistry in the tropical tropopause layer (TTL).
49   Most recently, UCATS completed the Atmospheric Tomography (ATom; 2016-18) mission, for which the
50   NASA DC-8 aircraft performed more than 600 vertical profile maneuvers over the Atlantic, Pacific and
51   Southern Oceans and parts of the Arctic and Antarctic from near the surface to above 12 km in different
52   seasons. Many of these missions required changes to UCATS, and components were also upgraded when
53   possible. The end result is a compact instrument for UAS and piloted aircraft, capable of measurements in the
54   stratosphere or troposphere, for studies of atmospheric composition, chemistry and transport. We describe
55   the basic configuration of UCATS in Sect. 2, subsequent improvements and modifications over the course of

Atmospheric
Measurement
Techniques
Discussions

1 its missions in Sect. 3, and data and intercomparisons from some of the field campaigns in Sect. 4, with a short
2 summary in Sect. 5.
3
4 **2 Overall instrument design**
5
6 At its core, UCATS is similar to previous gas chromatograph (GC) instruments designed and built for aircraft
7 and balloon platforms [Elkins et al., 1996; Romashkin et al., 2001; Moore et al., 2003]. It is primarily a two-
8 channel GC, packaged with small ozone and water vapor sensors in a compact design for small payload
9 spaces. Both GC channels use ECDs, with "dopant" gas as needed, to detect specific trace species with high
10 precision. In its original configuration, one channel used OV-101 in 3.2 mm O.D. packed columns to separate
11 and measure CFC-12, Halon-1211, and CFC-11 every 70 seconds, similar to the Lightweight Airborne
12 Chromatograph Experiment (LACE) [Moore et al., 2003]. After the initial Altair flights in 2005, this channel
13 was replaced by a pre-column of Unibeads and a main column of 5A molecular sieve to measure molecular
14 hydrogen (H_2), methane (CH_4), and carbon monoxide (CO) every 140 seconds. A tiny flow of nitrous oxide
15 (N_2O) dopant (~.003 sccm) added to the ECD is required to improve sensitivity. The second channel uses a
16 pre-column and main column of Porapak Q, followed by a post-column of 5A molecular sieve, to measure
17 sulfur hexafluoride (SF_6) and N_2O every 70 seconds; doping the nitrogen carrier gas with CO_2 enhances the
18 ECD response to N_2O.
19
20 Figure 1 shows a block diagram of UCATS with all the major internal components (only one GC channel is
21 included for clarity); more detailed drawings of the ozone and water instruments are included in the
22 appendix (Fig. A1a and A1b). Ambient air is drawn into UCATS from a side-facing or rear-facing inlet
23 extending 25-30 cm from the skin of the aircraft (outside the boundary layer) through stainless steel and
24 Synflex tubing; sample flow tubing inside the GC is stainless steel. Air is pressurized in the GC sample loops
25 by a two-stage KNF diaphragm pump (Model UN726, with Teflon-coated heads and diaphragms) and
26 maintained at 1225 hPa with an absolute pressure relief valve (Tavco, Inc.; Chatsworth, CA); excess air is
27 dumped through the Tavco overflow. Air flows at approximately 80 sccm sequentially through the two
28 sample loops (~0.5 cc volume, one for each channel) and a flow meter, and is controlled by solenoid valves
29 and a pressure regulator set at 1080 hPa on the outlet. Every 70 or 140 seconds the contents of the sample
30 loops are injected by 2-position Valco valves onto the pre-columns, providing a discontinuous ~2 second
31 "snapshot" measurement of ambient air.
32
33 The sample air flow is split just upstream of the GC pump to feed a tunable diode laser (TDL) hygrometer with
34 its own pump (KNF, model NMP850) downstream of the absorption cell. The original hygrometer, from
35 Maycomm, Inc., used infrared absorption at 1.37 μm with second harmonic detection to measure water vapor.
36 Since water vapor number densities span 5 orders of magnitude from the surface to the stratosphere, the
37 laser beam was split into two optical paths, a 13.4 cm "short path" for measurements from the surface to the
38 mid-troposphere (40,000 to 500 parts per million [ppm]), and a 403 cm multi-pass "long path" for
39 measurements from the mid-troposphere into the stratosphere (1000 to <5 ppm). On the Altair missions,
40 with a minimal payload, a small Vaisala probe was installed on the inlet for measurements of temperature,
41 pressure, and relative humidity. This was not used subsequently, as the payloads on larger aircraft included
42 dedicated instruments for meteorological measurements.
43

1
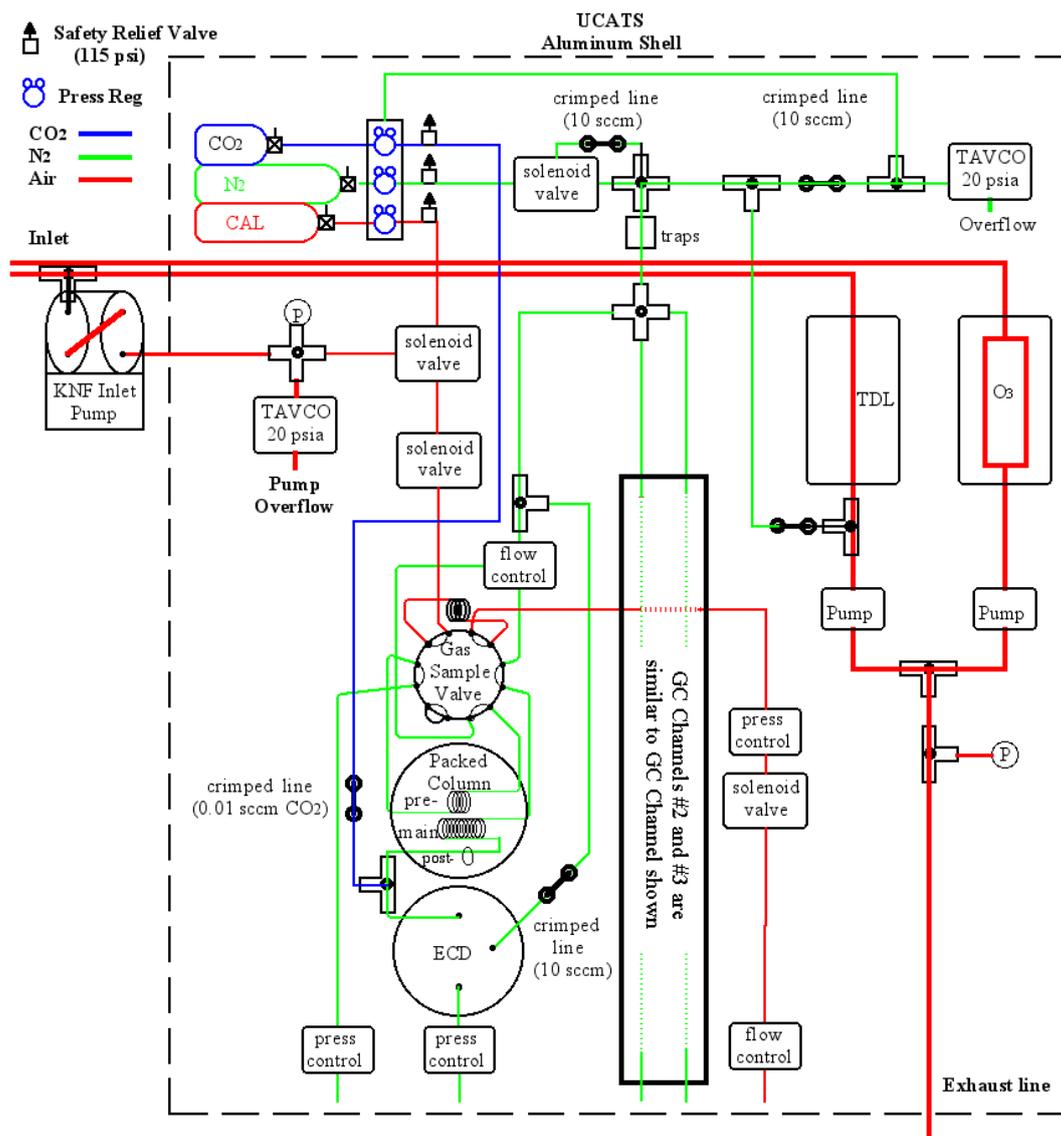
Figure 1: Schematic of UCATS showing all major components. Red lines indicate the flow of ambient air through the instrument and blue lines indicate ECD dopant flow. Only one GC (for N_2O and SF_6) is shown here for reference. All regulators ("Press Reg") are single-stage, and kept at a constant external pressure by a small flow of carrier gas and a second Tavco absolute pressure controller (green line, top) to improve stability. Pressure is measured at points in the system marked "P", as well as at regulators and controllers. Green "crimped lines" typically provide 5-10 cm^3/min purge flows to keep the ECDs and TDL cell clean and dry when the instrument is powered off, "make-up" flows to the ECDs when operating, and flows to pressurize the regulators. N_2 carrier gas (green lines) is purified through a set of molecular sieve, Hopcalite, and activated charcoal traps, and a hot zirconium getter, labeled as "traps" in the figure, before being sent to the GCs. Bottles for N_2 and calibrated air will be mounted inside the UCATS shell for the upcoming DCOTSS mission; they were previously located externally. Internal details of the ozone and water instruments are shown in Fig. A1a and A1b.

1 Ozone was measured by a series of direct absorption (Beer-Lambert Law) UV photometers from 2B
2 Technologies (Boulder, CO), modified for high altitude operation and mounted inside the UCATS package.
3 The initial ozone instrument was a 2B Model 205; modifications included a stronger pump (KNF, model
4 UNMP-830), a small metal cylinder upstream of the pump to dampen pressure fluctuations that could
5 degrade the measurement precision, O_3 scrubbers with manganese dioxide (MnO_2)-coated screens (Thermo
6 Fisher), and pressure sensors with a range from 0 to over 1000 hPa (Honeywell ASDX series). Ambient air
7 was brought to the ozone instruments from the inlet through a separate Teflon tube (6.35 mm O.D.) inside a
8 stainless steel jacket, with the exhaust from the ozone instrument(s) and the hygrometer combined inside
9 UCATS and released outside the aircraft. The Model 205 is a dual-beam photometer, with the flow
10 continuously split between unscrubbed (ambient) air into one cell and scrubbed (ozone-free) air into the
11 other. Two photodiodes located at the end of 15-cm long absorption cells measure the intensity of 254 nm
12 radiation emitted from a mercury lamp. Ozone concentrations are calculated from the ratio of measured
13 intensities through the cells with scrubbed and unscrubbed air according to the Beer-Lambert Law. The flow
14 paths are switched by solenoids every 2 seconds, to allow alternating measurements of ambient and
15 scrubbed air in each cell, with data averaged to 10 seconds on the original model. The instruments are
16 calibrated against a NIST-traceable calibration system (Thermo Fisher, Model 49i) on the ground before and
17 after every mission.
18
19 The overall dimensions of UCATS were initially 41 x 46 x 26 cm, with a weight of 29 kg. The external GC
20 pump weighs an additional 5 kg, and fiber-wrapped aluminum bottles (SCI Composites; now Worthington
21 Industries) for compressed nitrogen (N_2) carrier gas and dry, whole air calibration gas (injected every ∼9
22 minutes) for the GC together weigh approximately 7 kg. For flights on piloted aircraft, these can be replaced
23 by larger gas cylinders as weight and space allow. The total N_2 flow (carrier gas, backflush, purge flows) is
24 less than 300 sccm. UCATS is powered by 28 V DC, and the complete package draws 12 A at startup (∼350
25 W), decreasing to 150 W after the heaters warm up (∼30 minutes). UCATS is controlled by an Ampro
26 computer, and data are stored on flash memory for post-flight processing; "quick-look", near real time data
27 for ozone, water, N_2O, SF_6, and CH_4 are also provided by a serial or Ethernet connection to the aircraft, for
28 onboard use and telemetry to the ground.
29
30 **3 Field missions and modifications to UCATS**
31
32 **Table 1: Missions and configurations of UCATS. A second 2B Model 205 ozone instrument was added for ATTREX-**
33 **2 and 3. The water vapor instrument was converted to the newer Port City model for ATom-2 and subsequent**
34 **deployments. For the upcoming DCOTSS mission, UCATS is being repackaged to include three GC channels to**
35 **measure CFCs (CFC-11, CFC-12, and CFC-113) and H-1211; shorter-lived chlorine compounds ($CHCl_3$, CCl_4, and**
36 **C_2HCl_3); and N_2O and SF_6.**
37

Mission	Year	Aircraft	GC configuration	Ozone	Water vapor
UAS Demo.	2005	Altair	CFCs; N_2O/SF_6	2B 205	None
Western Fire	2006	Altair	$CH_4/CO/H_2$; N_2O/SF_6	2B 205	Maycomm
START-08	2008	GV	$CH_4/CO/H_2$; N_2O/SF_6	2B 205	Maycomm
HIPPO	2009-11	GV	$CH_4/CO/H_2$; N_2O/SF_6	2B 205	Maycomm
GloPac	2010	Global Hawk	$CH_4/CO/H_2$; N_2O/SF_6	2B 205	Maycomm
ATTREX	2011-15	Global Hawk	$CH_4/CO/H_2$; N_2O/SF_6	Two 205	Maycomm
ATom	2016-18	DC-8	$CH_4/CO/H_2$; N_2O/SF_6	2B 211	Port City
DCOTSS	2021-23	ER-2	3 channels, see caption	2B 211	Port City

38
39 Aircraft missions that included UCATS are summarized in Table 1 and described in this section. The first two
40 projects were designed to show that high-quality measurements could be made on a UAS with autonomous
41 instruments. The NOAA/NASA UAS Demonstration Project using General Atomics' Altair (Predator B-ER)
42 UAS was conducted from the General Atomics flight facility at Gray Butte, CA, during April-May and
43 November, 2005. UCATS measured N_2O, SF_6, CFC-11, CFC-12, and halon-1211 with the two GC-ECD channels,
44 and ozone with the UV photometer. Including test flights, more than 63 hours of atmospheric composition

Atmospheric
Measurement
Techniques
Discussions

1   data were acquired up to altitudes of 13 km. The mission highlight, an 18.4-hour flight over the eastern
2   Pacific Ocean, successfully demonstrated that atmospheric composition and other environmental parameters
3   can be measured with high precision and accuracy from a UAS [Fahey et al., 2006].
4
5   The NASA/USDA-FS/NOAA Western Fire mission was conducted in August and October, 2006, again using the
6   Altair UAS [Hinkley et al., 2009]. The scientific focus was predominantly on improving the remote mapping of
7   wildfires from a UAS, with UCATS onboard to measure atmospheric trace gases in fire plumes. For this
8   mission, the GC-ECD halocarbon channel was replaced with an N_2O-doped GC-ECD channel designed to
9   measure the combustion products CO and CH_4, along with H_2. A TDL-based water vapor sensor was added to
10   UCATS for this and future missions. Accomplishments of this project included 21- and 22-hour science flights
11   and more than 65 hours of UCATS *in situ* measurements of trace gases and water vapor.
12
13   For START-08 [Pan et al., 2010] and HIPPO [Wofsy, 2011], both UCATS and the PAN and Trace
14   Hydrohalocarbon ExpeRiment (PANTHER), a four-channel GC with ECD detection and a GC with mass
15   spectrometry detection (GC/MS), were flown on the NSF/NCAR GV aircraft. These were integrated together
16   with a NOAA whole air sampler (WAS) in collaboration with the University of Miami [Schauffler et al., 1999].
17   The larger GV payload was designed to probe long-lived greenhouse gases and tracers of atmospheric
18   transport. In HIPPO, the GV flew repeated vertical profiles between 150 m above sea level and 14 km, largely
19   over the Pacific Ocean, from northern Alaska and the Arctic Ocean to south of New Zealand near Antarctica,
20   with five deployments from January 2009 to August 2011 covering different seasons. The first use of UCATS
21   in the extremely humid tropics during HIPPO revealed several issues, which were resolved after the first two
22   deployments. Initially, the GC columns adsorbed water, which changed their retention characteristics. To
23   prevent this, a Nafion dryer [Perma Pure, MD-050-72S-2] was added to desiccate the sampled air, with the
24   exhaust from the pre-columns used as the dry counterflow gas. The Nafion dryer helped considerably, but
25   retention times and sensitivity for the N_2O/SF_6 channel still showed changes after passing through very
26   humid air. The problem was finally resolved by lengthening the 5A molecular sieve post-column from ~20 to
27   25 cm. This allowed the post-column to be operated at 190 °C instead of 115-120 °C, with similar retention
28   times. Water does not accumulate at the higher temperatures and the chromatography remained constant.
29   The peaks also sharpened considerably, requiring changes to the electrometer circuit board to achieve a
30   faster response time and avoid saturation of the signal. These were completed in 2015, prior to the ATom
31   mission. Plots illustrating data quality and intercomparisons are shown in Sect. 4.
32
33   Problems were also identified with the 2B ozone instrument during the START-08 and HIPPO missions. As
34   the GV passed through regions of high humidity (>1000 ppm water vapor) and then back into drier air, the 2B
35   instrument produced anomalous ozone readings compared to a direct absorption instrument operated by the
36   NOAA Chemical Sciences Laboratory (CSL). UV ozone photometers are known to suffer from offsets when
37   transitioning between wet and dry conditions [Wilson and Birks, 2006], because of water being retained in
38   the scrubber and slowly released, differentially affecting reflectance from the walls of the cell with scrubbed
39   air compared to the cell with ambient air. This was resolved for the ATom mission, as described later in this
40   section.
41
42   From 2010 to 2014, UCATS was integrated into a compartment in the fuselage of the NASA Global Hawk UAS
43   for the GloPac and ATTREX missions [Jensen et al., 2013]. The Global Hawk generally operates in the
44   stratosphere and upper troposphere (12-20 km), where air is very dry. However, these missions led to other
45   changes in order to improve signal-to-noise for ozone. The original 2B Model 205 could achieve a precision of
46   ±2% + 1 part per billion (ppb) with 10 second averaging at atmospheric pressure. Because Beer-Lambert
47   absorption is really a measurement of number density (concentration) of the absorbing molecule, the
48   precision varies inversely with pressure (1 ppb precision at 1000 hPa corresponds to a precision of 10 ppb at
49   100 hPa, a typical pressure in the UT/LS). This is more than adequate for midlatitude and polar stratospheric
50   missions such as GloPac, where ozone varies from a few hundred to a few thousand ppb. But for ATTREX,
51   where the focus was the tropical tropopause layer (TTL; Fueglistaler et al., [2009]), ozone was typically less
52   than 100 ppb, at pressures of 150-70 hPa. To partially address this issue in ATTREX-2 and 3 (2013-14), a
53   second Model 205 sensor was added to UCATS. The original Model 205 remained completely enclosed and
54   the new one was added to the front panel, with part of the instrument inside the sheet metal UCATS enclosure
55   and the cell, lamp, and detectors on the surface, with a small insulated cover and warm airflow from UCATS

Atmospheric
Measurement
Techniques
Discussions

1 passing through it. In general, the older 2B had better stability over a flight, possibly because of the more
2 constant temperature environment inside UCATS. However, after a few hours of operation (always the case
3 with Global Hawk flights, which could last for ~24 hours with the ATTREX payload), both instruments
4 converged to stable and consistent readings. When both instruments were operating normally, data from the
5 two instruments were merged and averaged to create a combined data set with a value reported every 5
6 seconds. UCATS served as the primary ozone instrument during ATTREX-3, where weight and balance issues
7 with the payload prevented the NOAA CSL instrument from being flown on the Global Hawk.
8
9 The ATom mission was similar to HIPPO, but with a much larger payload to map out and study atmospheric
10 chemistry as well as long-lived gases over remote regions. For ATom, a new 2B Model 211 ozone photometer
11 was added to UCATS and the partially external Model 205 removed. The Model 211 has a longer cell and path
12 length (30 cm compared to 15 cm for the Model 205), improved electronics, and built-in flow meters to
13 assure equal flows through each cell, with a stated precision that is the sum of 1% + 0.5 ppb over a 10-second
14 average at 1000 hPa. As purchased, it used photolysis of N_2O to produce NO as the scrubber; this method is
15 not affected by changes in humidity of the sampled air. However, at high altitudes, with fixed addition of N_2O
16 (or NO), the concentration of NO decreases with decreasing pressure in the instrument, and the rate of the
17 chemical reaction ($NO + O_3 \rightarrow NO_2 + O_2$) that removes ozone decreases proportionally. Rather than trying to
18 add more NO to compensate (carrying toxic gases like NO on an aircraft is problematic; even large amounts of
19 an oxidizer such as N_2O add to the complexity of getting a payload certified), we used a conventional scrubber
20 (MnO_2-coated screens) and passed both the scrubbed and ambient airflows through the Nafion moisture
21 exchangers provided with the instrument. Moisture exchangers have been shown to eliminate the artifacts
22 associated with rapid changes in water vapor by keeping both cells at a constant humidity [Wilson and Birks,
23 2006]. They were not used for HIPPO and START-08, because the pressure of the gas flow being analyzed
24 varied from ~100 to 1000 hPa while the cabin pressure was maintained near 900 hPa at high altitudes for the
25 people on board. With a pressure differential of over 700 hPa, the soft Nafion tubes could leak or collapse and
26 block the flow. We solved this potential problem in ATom by placing the Nafion tubes in a small aluminum
27 box (McMaster-Carr, 75895K series), sealed to the outside except for a small flow (50-200 sccm) of moist air
28 (cabin air passed through a short piece of 12.7 mm dia. tube containing wet cotton) through the box and into
29 the exhaust line from the ozone instrument. Thus, the pressure inside and outside the Nafion tubes stayed
30 approximately equal. This simple solution eliminated the effects of rapid changes in humidity, as
31 demonstrated by comparisons with another ozone instrument (see Fig. 9 and 10 below).
32
33 The TDL hygrometer in UCATS was also upgraded during ATom with a new model from Port City Instruments
34 (Reno, NV), the successor to Maycomm. It is similar in concept and uses a distributed feedback laser (DFB) to
35 scan across two closely spaced absorption lines near 2.574 μm. Absorption at this wavelength is much
36 stronger than in the original instrument, allowing higher sensitivity in the stratosphere. As before, the laser
37 beam is split into two optical paths, with the short path (5.14 cm) for high values of tropospheric water
38 (~2000-40000 ppm) using direct absorption. The long path (280.0 cm) is used with second harmonic
39 detection for water vapor from 0-100 ppm, and intermediate values (100-5000 ppm) are measured using the
40 long path with direct absorption. A second weak absorption line is also analyzed with direct absorption for
41 water vapor mixing ratios above 1000 ppm; this is not being used at present. Both long and short path
42 spectra are recorded simultaneously, with each scan taking approximately 200 msec. All four measurements
43 of water vapor are calculated, then each is averaged together for ~1 Hz output on a serial data line. All data
44 are recorded by the UCATS computer and the appropriate value for display and archiving is chosen based on
45 the range of pressure and water vapor. Both instruments required extensive calibration using prepared
46 water vapor standards and frost point hygrometers for accurate measurements. The new instrument allows
47 higher precision (±0.1 ppm or better) measurements of water vapor in the stratosphere compared to the
48 original instrument, which was limited to ±1 ppm.
49
50 Both the new ozone and water instruments were larger than the original models, and could not fit into the
51 existing UCATS shell. A 7.5 cm extension was added to the top of UCATS, with the new water and ozone
52 instruments and main cooling fans secured to the top plate. The original 2B Model 205 ozone instrument was
53 left on the side to enable a comparison of results, and to provide a known and reproducible pressure
54 measurement when needed. The total weight increase was about 5 kg, but this is negligible on an aircraft
55 with the size and capacity of the DC-8.

4 Data intercomparisons and discussion

In this section, we present results in the stratosphere first, then in the troposphere. To compare with UCATS, we used data from many other instruments. On the GV, the Quantum Cascade Laser Spectrometer (QCLS; Santoni et al., 2014) measured long-lived trace gases, including N_2O and CH_4, with high precision and 1-second time resolution, ideal for comparing time series and tracer-tracer correlation plots. The PANTHER instrument (a 4-channel GC, with a separate GC/mass spectrometer) also measured the same molecules by GC as UCATS, using similar techniques. Whole air samples were collected in glass flasks using Programmable Flask Package units (PFPs), which could be filled on demand or in a preset sequence, with 24 samples typically collected per flight. Samples were later analyzed at the NOAA Global Monitoring Laboratory for a large set of trace gases [Sweeney et al., 2015]. All these instruments were also on the DC-8 aircraft for the ATom mission. Data from the Airborne Chromatograph for Atmospheric Trace Species (ACATS; Elkins et al., 1996), a predecessor of both PANTHER and UCATS, are also used from the 1997 Photochemistry of Ozone Loss in the Arctic Region in Summer (POLARIS) mission for comparison.

The NOAA Chemical Sciences Laboratory (CSL) "Classic" ozone instrument [Proffitt and McLaughlin, 1983] has a long history of measurements on high altitude aircraft, and flew on the GV during HIPPO. This was replaced with a new lighter version, "NOAA-2" [Gao et al., 2012] for Global Hawk missions. A different group from NOAA CSL flew a chemiluminescence ("CL") instrument on the DC-8 in ATom for measurements of ozone [Bourgeois et al., 2020], NO, NO_2, and total reactive nitrogen (NO_y). Ozone data from concurrent GML sonde launches [Komhyr et al., 1995] and the NCAR chemiluminescence instrument [Ridley et al., 1992], on the GV during the Convective Transport of Active Species in the Tropics (CONTRAST) mission, were also used for ATTREX data comparisons and analysis.

The diode laser hygrometer (DLH; Diskin et al., 2002; Podolske et al., 2003), an open-path near-infrared absorption instrument, whose optical path is defined by a transceiver in the fuselage and a retroreflector mounted below one of the wings, was used to measure water vapor on the Global Hawk and DC-8. During ATTREX, the NOAA CSL TDL hygrometer (also built by Port City) also measured water vapor. The Meteorological Measurement System (MMS; Scott et al., 1990) was used on the Global Hawk and DC-8 missions for position and meteorological variables.

4.1 Gas Chromatographs

Global Hawk flights during the GloPac mission covered a wide range of air masses in the stratosphere, and provided an opportunity to demonstrate the capabilities of UCATS in the environment for which it was designed. Figure 2 shows a correlation plot of SF_6 vs. N_2O mole fractions for the flight of April 23, 2010, from Edwards AFB, CA to the western Arctic Ocean and back (~35-85 °N, 120-165 °W) at altitudes from 16 to 20 km, with two profiles down to 13 km and back. N_2O and SF_6 are long-lived greenhouse gases emitted at Earth's surface, and generally decline with altitude in the stratosphere [e.g., Plumb and Ko, 1992]. For N_2O this is primarily because of photochemical loss in the stratosphere, and for SF_6 it is primarily because older air entered the stratosphere at earlier times, when tropospheric SF_6 mixing ratios were lower [Hall et al., 2011]. As a result, N_2O and SF_6 are correlated in the stratosphere, with older air and air from higher altitudes having the lowest mixing ratios for both gases. This correlation can be seen in Fig. 2, where N_2O declines strongly from its tropospheric value (~320 ppb in 2010) as SF_6 (tropospheric value 7.0 ppt in 2010) approaches 5.5 ppt. Data from ACATS-IV taken on the ER-2 aircraft almost 13 years earlier in the Arctic during the 1997 POLARIS mission are shown on top of the GloPac data. POLARIS N_2O and SF_6 mixing ratios were adjusted upward for the tropospheric growth over the 13 years between missions (N_2O increased from 312.5 to 322.9 ppb, and SF_6 from 3.9 to 7.0 ppt) by adding the difference in tropospheric values to the POLARIS data. The measurement precision for UCATS is about ±0.04 ppt SF_6 (1 σ) and ±1 ppb N_2O, similar to ACATS, with the data close to overlapping, as expected. The slightly more gradual slope of the correlation plot for POLARIS is due to the fact that SF_6 was increasing more slowly in the 1990's than in the years just before GloPac [Hall et al., 2011]. Similar plots of GloPac and (adjusted) POLARIS CH_4 vs N_2O and H_2 vs CH_4 data from the same flights (Fig. 3) show excellent agreement between the two campaigns and tight, nearly linear correlations, as expected from the fact that these are all long-lived gases in the stratosphere. Overall,

Atmospheric
Measurement
Techniques

Open Access

EGU

Discussions

1 UCATS precision for CH_4 and H_2 was ±7-8 ppb (0.5%) and ±5 ppb (1%) respectively, equal to or better than
2 that of ACATS-IV.
3
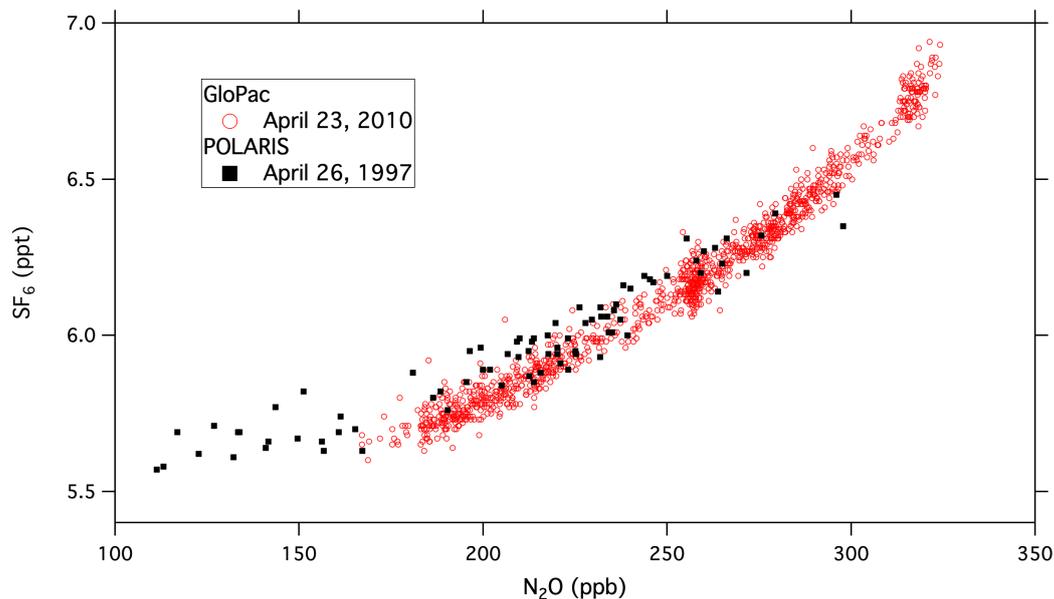
4
5
6 **Figure 2: UCATS SF_6 plotted vs. N_2O from the GloPac mission (red circles), with similar data from ACATS (black**
7 **squares) during the POLARIS mission 13 years earlier. The POLARIS data have been adjusted for the**
8 **tropospheric increases in both gases between 1997 and 2010 (see text). The GloPac correlation has a slightly**
9 **steeper slope than for POLARIS, reflecting the increased growth rate of SF_6 during and prior to GloPac.**
10
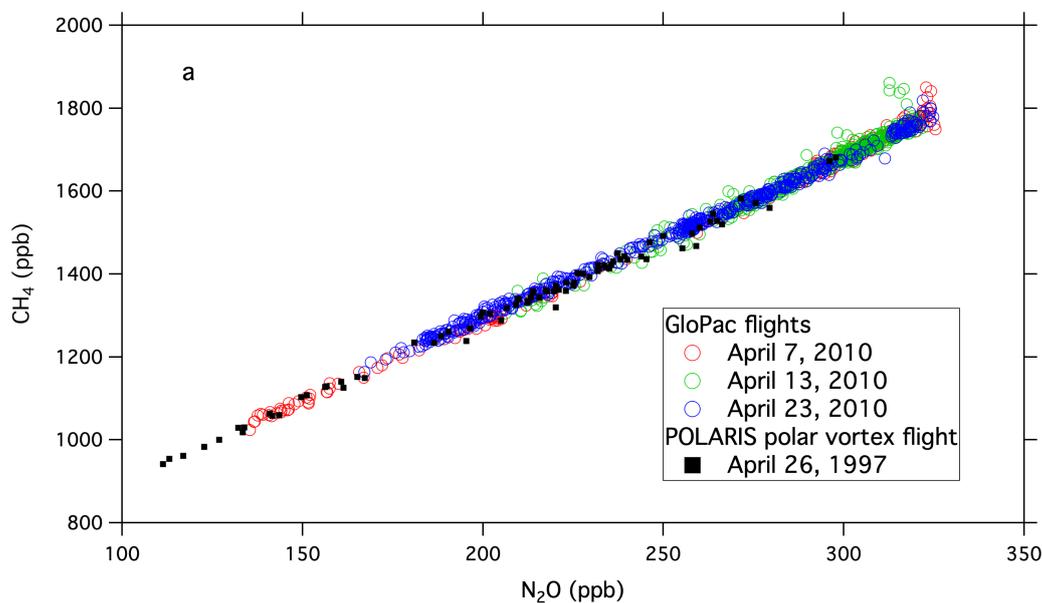
11
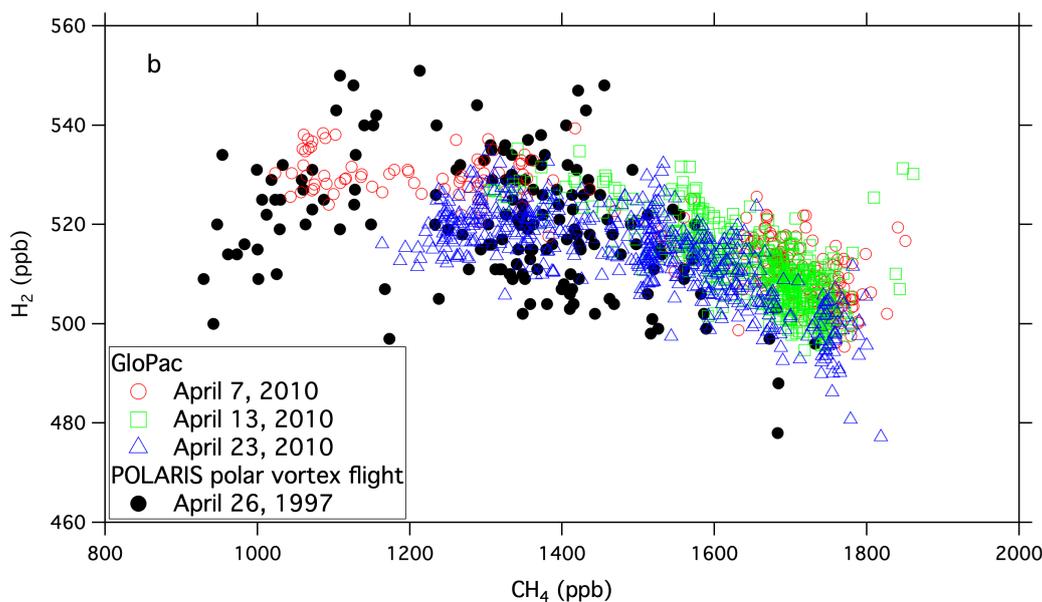
Figure 3: Similar correlation plots to Fig. 2, showing CH$_4$ vs. N$_2$O (a) and H$_2$ vs. CH$_4$ (b). Molecular hydrogen increases slightly in the stratosphere from CH$_4$ photooxidation, leading to their anticorrelation.

The START-08 and HIPPO missions were the first tropospheric campaigns for UCATS. On January 12, 2009, during the first HIPPO deployment, the GV sampled air in both the troposphere and stratosphere as it traveled from Anchorage, AK, north to near 80 °N over the Arctic Ocean, and back. The precision for UCATS N$_2$O during most of the flight was near ±1 ppb in both the troposphere and stratosphere, calculated from flight segments with near-constant N$_2$O near the start of the flight, and comparisons with QCLS and PFP samples throughout the flight (Fig. 4a). A more quantitative comparison can be made by plotting UCATS and PFP data for the entire HIPPO 1 deployment against the higher time resolution QCLS data (Fig. 4b). Each UCATS GC measurement (every 70 seconds for N$_2$O and SF$_6$) is a roughly 2-second average of the atmospheric composition along the flight path a few seconds before the air sample is injected, and is plotted here against the corresponding 10-second average of QCLS data. Each PFP flask takes between 30 seconds and a few minutes to fill, depending on altitude, and a comparison with QCLS data is enabled by averaging the QCLS data over the sampling interval associated with each flask sample. The UCATS vs. QCLS correlation allows an upper limit estimate of UCATS precision, assuming all the error is associated with the UCATS measurements, none from QCLS, and that effects related to atmospheric variability arising from timing mismatches are negligible. The resulting standard deviation (1-σ precision) is ±1-2 ppb over the entire month of HIPPO flights, from the high Arctic through the tropics to the Southern Ocean and back. The slope of the fit is 0.91 ± 0.004; this difference could be due to nonlinearities in one or both of the instruments and has not been resolved. We note that the slope for the PFP data is 0.93 ± 0.02, though this is partially driven by the smaller slope for tropospheric (high N$_2$O) data, as opposed to for UCATS, where the slope is also smaller in the troposphere but clearly driven by differences in the stratosphere (low N$_2$O), where the dynamic range of N$_2$O is large. The UCATS and PFP results agree closely over the more limited range of PFP N$_2$O data, but because the measurements were not simultaneous, a quantitative comparison is not possible. Although UCATS was able to produce precise and accurate data, the chromatography was not stable over the course of the HIPPO deployment as the GC columns picked up and retained water, especially in the tropics. As described above, this was addressed before HIPPO-4 by adding a Nafion dryer to remove most of the water from air samples, lengthening the post-column for N$_2$O and SF$_6$ and increasing its temperature to prevent it from retaining residual water, and eventual improvements to the electronics for faster time response while maintaining linearity of peak heights vs mixing ratio.
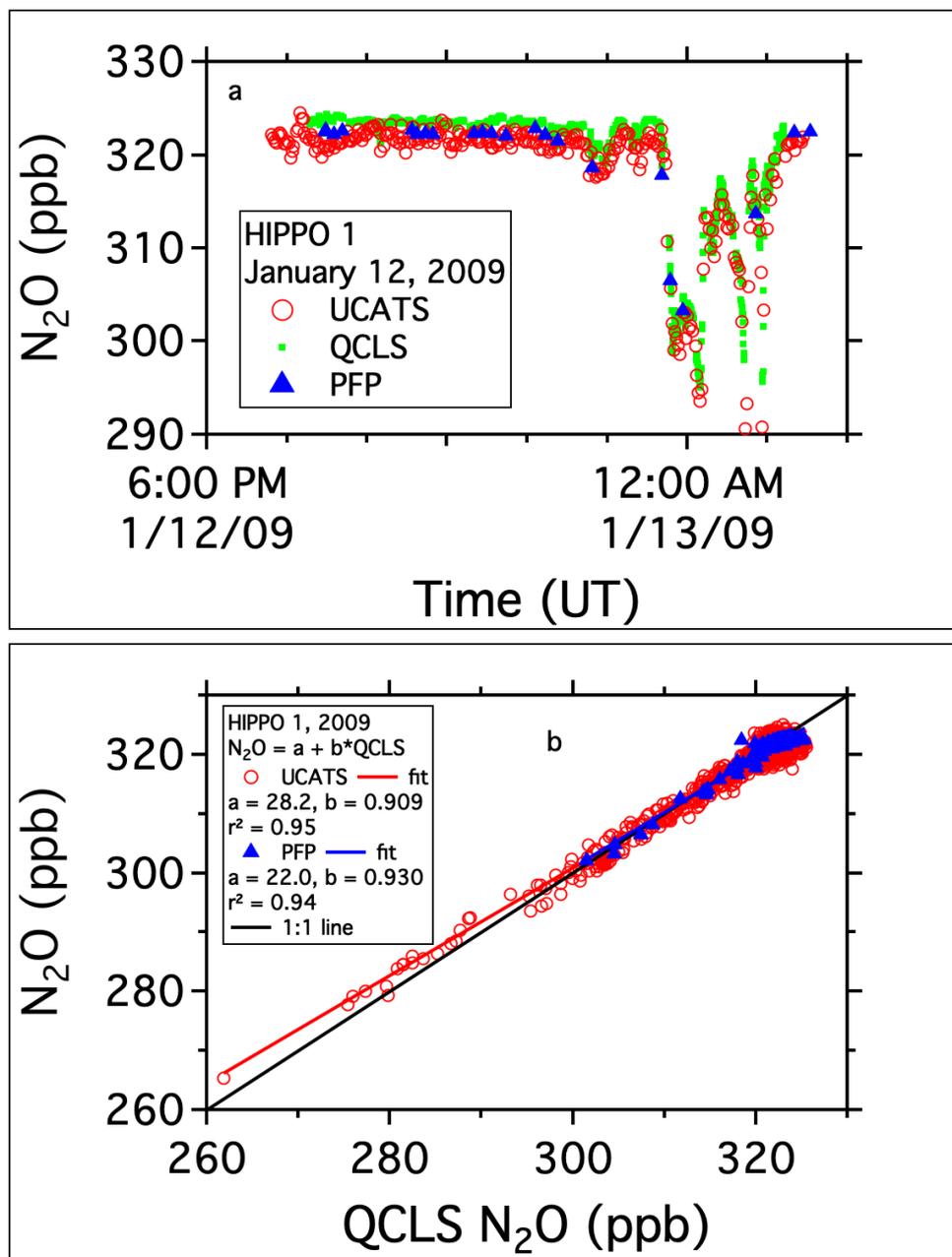
3 **Figure 4:** N$_2$O data from the HIPPO mission on the GV aircraft. Panel (a) shows the time series from a flight north
4 from Anchorage, AK over the Arctic Ocean and back. The aircraft flew several profiles from 14 km to near the
5 surface during the flight. Panel (b) shows UCATS and PFP data plotted against QCLS data over the entire
6 deployment.
7
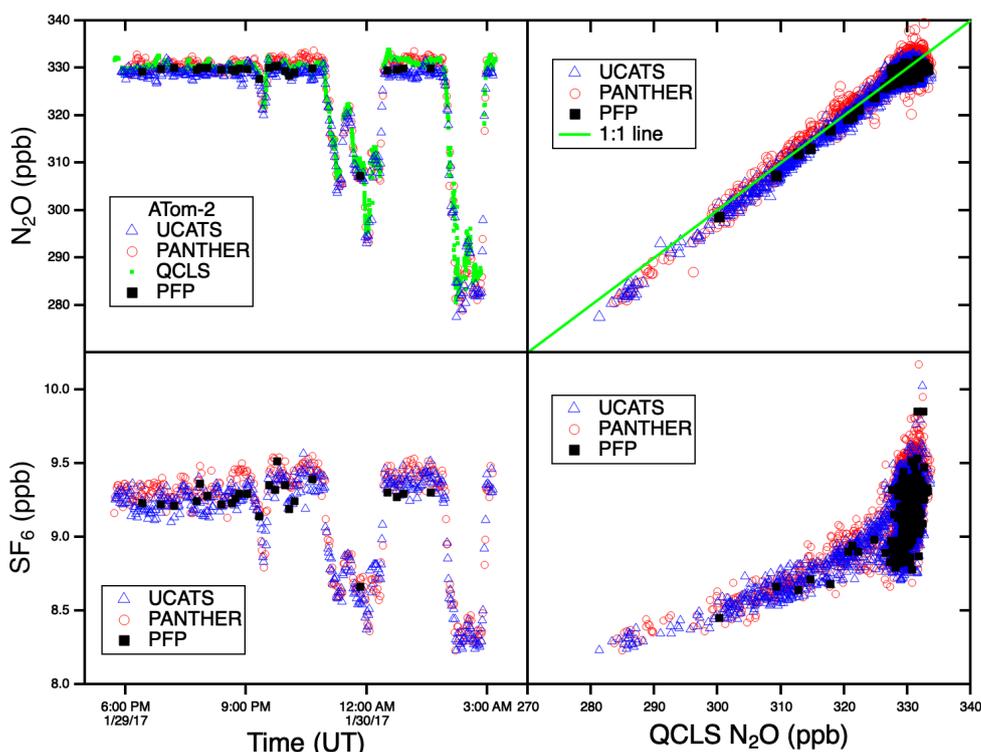
Figure 5: N_2O and SF_6 time series for one flight (left), and scatter plots for all the NOAA instruments against QCLS N_2O data from the entire ATom-2 deployment (right). The flights, from January 26 to February 21, 2017, spanned the Pacific, Atlantic and Southern Oceans, and the Arctic. With improvements to the N_2O/SF_6 channel, UCATS was able to achieve similar precision to the HIPPO-1 data shown in Fig. 4, but without the instability driven by accumulated water in the GC columns. N_2O and SF_6 do not have a simple relationship in the troposphere, so the panel on the lower right does not yield a single curve as in Fig. 2.

In ATom, with all these changes in place and optimized, UCATS was able to produce precise and accurate GC data in the troposphere with both short and long-term stability and without degradation in the humid tropics. This is demonstrated by N_2O and SF_6 time series for the DC-8 flight of January 29, 2017, from Palmdale, CA to northern Alaska, and back to Anchorage (~35-70 °N, 120-155 °W), and scatter plots for the entire ATom-2 deployment (Fig. 5). Data from UCATS, PANTHER, QCLS (N_2O only), and PFPs show excellent agreement for the time series (mean differences typically ±1-2 ppb N_2O and ±0.05 ppt SF_6). The 1-σ precision of UCATS and PANTHER was ~±1 ppb N_2O and ±0.05 ppt SF_6 from both the time series and the scatter plots (again assuming all the variability in the comparison with QCLS is associated with the GC data). SF_6 and N_2O are not particularly well correlated in the troposphere, so the precision of SF_6 from the lower right panel can only be estimated for stratospheric data. The only disagreement is at low values of N_2O, where PANTHER and UCATS both measure about 3 ppb lower than the QCLS instrument. The tropical flight of February 3, 2017 (Fig. A2) illustrates the precision of N_2O and SF_6 where air masses sampled along the flight track varied slowly (because of its altitude range, the DC-8 is always in the troposphere at these latitudes). H_2 measurements also showed good agreement between UCATS, PANTHER, and PFPs (Fig. 6), with nearby data points from the different instruments typically differing by about ±5 ppb (1%) over the entire range of observed values. Values for precision and agreement of measurements from ATom and other missions are summarized in Table A1.

Atmospheric
Measurement
Techniques
Discussions
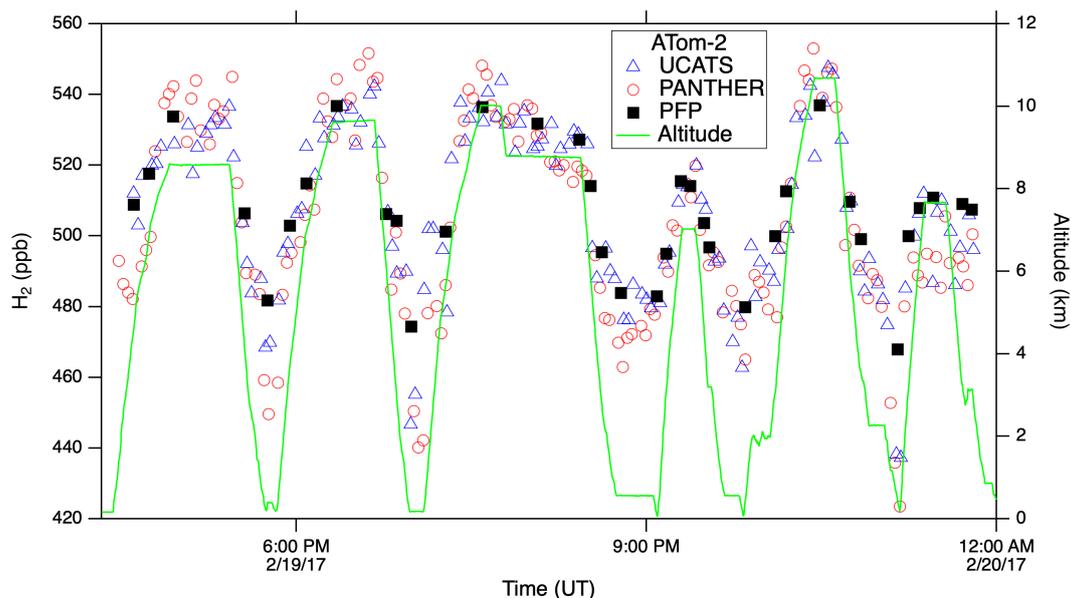
Figure 6: H$_2$ from UCATS, PANTHER, and PFPs showed close agreement in the troposphere and lower stratosphere during ATom. Because of the dominant soil sink for H$_2$, mixing ratios are lower near the surface, as seen on this flight from Thule, Greenland to Anchorage, AK, over the Canadian Arctic, the Arctic Ocean, and Alaska.

4.2 Ozone - stratosphere

This section is primarily focused on the ATTREX mission, which was designed to probe the chemical composition of air over the tropical Pacific and transport into the stratosphere, but applies to all UCATS stratospheric data. Because ozone mixing ratios peak in the stratosphere, the main requirements for a stratospheric ozone measurement are accuracy and stability, with sensitivity to low values usually less critical. In GloPac, the 2B Model 205 in UCATS agreed within 1% with NOAA Classic over the large observed range of ozone mixing ratios (Fig. A3). Requirements are different in the tropical tropopause layer (TTL), however, where ozone mixing ratios are very low, often less than 30 ppb. Both measurement accuracy and precision are essential at these low values, and even errors of a few ppb in ozone (or small measurement biases in water vapor and other trace gases) can lead to different interpretations of the underlying atmospheric processes. This put a stringent requirement on the quality of our ozone measurements for ATTREX. The 2B Model 205 is a small, lightweight, low-cost and low-power instrument, with a precision of about ±1 ppb at sea level. However, as discussed previously, at 100 hPa (near the middle of the TTL) this corresponds to a precision of ±10 ppb, which can be 50% or more of the measured mixing ratio in this region. The accuracy of the Model 205 ozone instrument can be calculated similarly to Proffitt and McLaughlin (1983), where the most important uncertainties are the absorption cross-section of ozone, the accuracy of cell temperature and pressure measurements, and the absorption path length. These add up to a few percent, but the calibration of the 2B instruments against a NIST reference standard should account for any slight inaccuracies. For all calibrations, the slope was within 1% of unity and the offset less than 2 ppb (usually <1 ppb), at ambient pressure (~840 mbar in Boulder, CO, and 920 mbar in California) and room temperature.

As described in Sect. 3, two Model 205 sensors were flown in UCATS during ATTREX-2 and 3, with data from the two instruments merged to improve precision. A comparison of UCATS and NOAA-2 ozone data from ATTREX-2 (Fig. 7) shows that the slope is close to unity with a crossover point near 500 ppb. At low ozone (20-30 ppb), the UCATS data are on average lower by 3-4 ppb. Since the absorption cross-sections are the same for both instruments and cell length is fixed (and measured to better than 1% accuracy), the principal

1   known sources of error are inaccuracies in measured cell temperature and pressure. The pressure sensor in
2   the older 2B instrument was carefully calibrated over a range of pressures for many years (2010-2016), and
3   was stable throughout that time. A small correction was made to account for the pressure drop from the cell
4   to its outlet (where pressure is measured). This introduced about a 1% increase in ozone at the highest
5   altitudes but was negligible at lower altitudes. Temperature is measured on the cell body rather than in the
6   airflow, but air temperature should have time to equilibrate inside UCATS before reaching the ozone
7   instruments. (Flow to each 2B is ~10% of that for NOAA-2, which has been shown to measure temperature
8   accurately after warming ambient air as it flows to the cell [Gao et al., 2012].) The offset between NOAA-2
9   and 2B data bears further examination. UV ozone photometers have been shown to produce offsets when
10   transitioning from wet to dry conditions (Wilson and Birks, 2006), and that is certainly the case for the Model
11   205, as discussed in the following section. However, except on initial ascent, air sampled in ATTREX was
12   always extremely dry, and any artifact should become negligible within 1 hour. Similar agreement between
13   NOAA-2 and the original 2B instrument was obtained on ATTREX-1 and the Global Hawk Pacific (GloPac)
14   mission in 2010. Laboratory tests for measurement artifacts of the 2B under various conditions produced
15   mostly negligible offsets, and always less than 5 ppb.
16
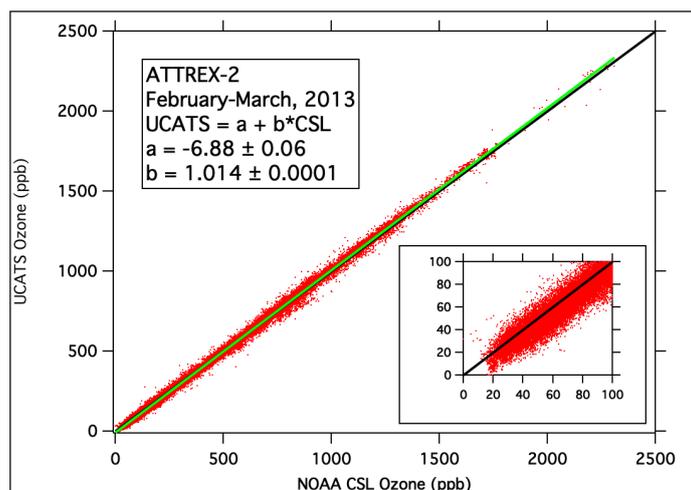
17
18
19   **Figure 7: Merged UCATS ozone data from the two 2B Model 205 instruments plotted against coincident data from**
20   **the NOAA Chemical Sciences Laboratory NOAA-2 ozone instrument for all six research flights during ATTREX-2 in**
21   **2013. The green line is the least squares fit to the data (parameters shown in the legend) and the 1:1 line is**
22   **shown in black. The inset shows ozone values <100 ppb.**
23
24   During ATTREX-3, issues with payload weight and balance prevented the NOAA-2 instrument from being
25   flown on the Global Hawk. Coincident balloon-borne electrochemical concentration cell (ECC) ozonesonde
26   launches from Guam provide a comparison for these flights. Data from the last 2 hours of the February 16-17,
27   2014 Global Hawk flight (Fig. 8) most closely overlapped one of the balloon profiles in space and time (within
28   100 km and 1-2 hours). The agreement between the ECC and the 2B instruments in the troposphere (<16 km,
29   where the balloon and aircraft were in closest proximity) is quite good and shows no significant bias in the
30   UCATS data. A further check on UCATS ozone is shown in Fig. A4 with ozone data from the GV aircraft
31   (operating during the concurrent CONTRAST mission; Pan et al., 2017), the Global Hawk, and the Guam
32   ozonesonde launch, which was timed to overlap with the return of the Global Hawk on February 13. In
33   summary, based on laboratory calibrations, tests, and in-flight comparisons, we assign a systematic
34   uncertainty of less than 5 ppb to our Model 205 ozone data in the TTL and lower stratosphere. The precision
35   in the TTL ranged from ±5 to 10 ppb but can be improved by temporal averaging. The low values of ozone in
36   the TTL demonstrate the importance of precise and sensitive ozone measurements in this region and the
37   need to minimize or eliminate any systematic errors.

Atmospheric
Measurement
Techniques
Discussions
Open Access
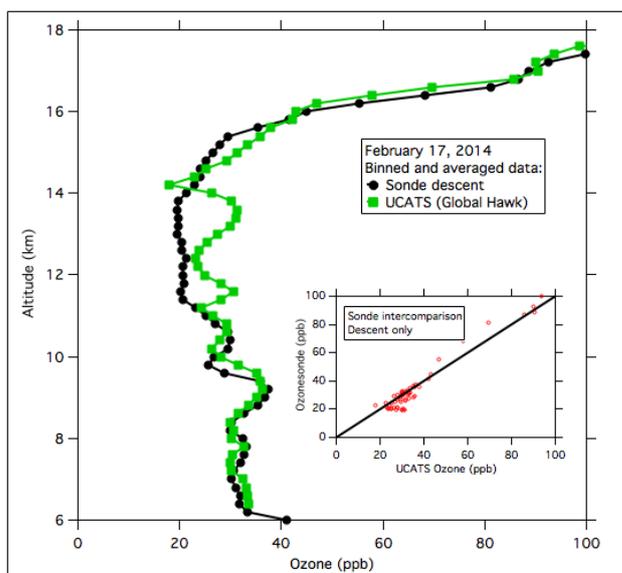
Figure 8: UCATS and ozonesonde data from February 17, 2014 near Andersen AFB, Guam. UCATS data (solid green squares) from the last part of the flight are binned and averaged by altitude; the solid black circles are the binned and averaged sonde descent data from near when the Global Hawk landed. The inset shows a scatter plot of binned UCATS and sonde data at coincident altitudes; the 1:1 line is shown in black.

4.3 Ozone - troposphere

As described above, the Model 205 in UCATS disagreed with the NOAA "Classic" instrument during HIPPO following transitions between wet and dry air. Most flights had only minor artifacts, but the issue was most pronounced in the tropics, with an example shown in Fig. 9 (top). At low altitudes there was generally good agreement (mean difference = 0.4 ppb, standard deviation = ±4.2 ppb for HIPPO 4), but as the GV aircraft climbed out of the very wet lower troposphere to higher altitudes, changes in water retained in the scrubber likely affected the reflected light along the sides of the cell, causing an anomalously high ozone signal. Even though flows are greater than 1 liter/min., the instrument took 15 minutes or more to recover. In ATom, with the newer Model 211 instrument and moisture exchangers for both scrubbed and unscrubbed air, the agreement was much closer over a similar flight track, and there were no anomalous data segments as the DC-8 ascended and descended (Fig. 9, bottom). The one discrepancy is in the tropical marine boundary layer (MBL), where UCATS was typically a few ppb higher than the chemiluminescence instrument. This disagreement is outside the combined uncertainties of the two instruments and is not currently understood; UCATS showed no differences when calibrated with wet or dry air in the laboratory, and the effect of water vapor on the chemiluminescence instrument has recently been re-checked. There were no offsets in the high latitude MBL (agreement within 1 ppb), so it is presumably related to the high humidity or something else present in the tropical MBL.
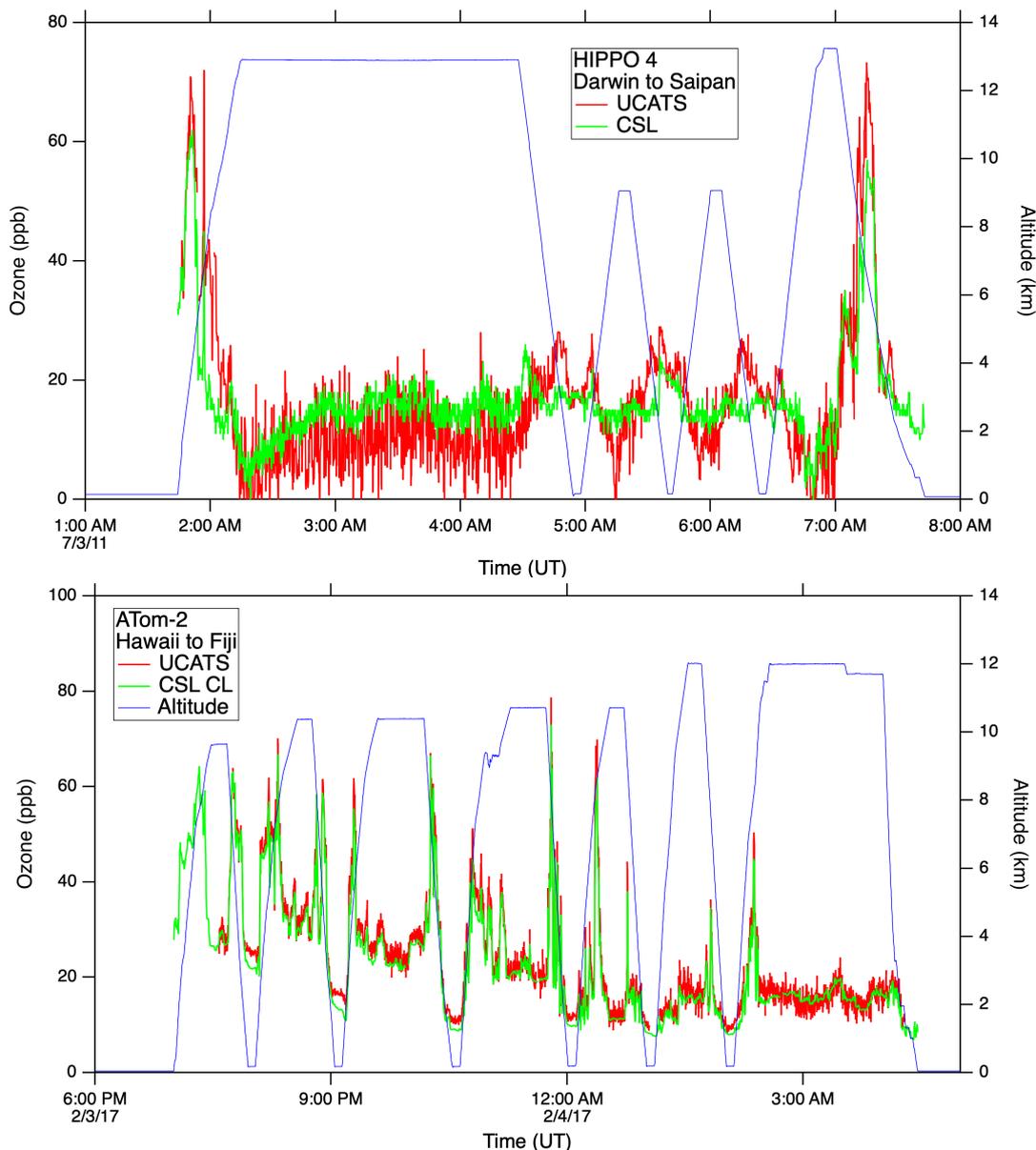
Figure 9: Ozone time series from HIPPO (top) and ATom (bottom). The upper plot shows an example of the discrepancies between the 2B Model 205 and Classic Ozone instruments observed in the tropics during HIPPO; extratropical flights were in closer agreement. The lower plot shows ATom data (over a similar range of latitudes) from the NOAA chemiluminescence instrument and the UCATS Model 211 ozone instrument, modified with moisture exchangers to ensure that air to both cells remained at reasonably high humidity.

Scatter plots of UCATS ozone data against the corresponding instrument from NOAA CSL (Fig. 10) showed reasonable overall agreement in HIPPO, with the slope within 1% of unity. But in HIPPO, there are many UCATS data points in the troposphere with significantly higher ozone than measured by the Classic Ozone

1 instrument (e.g., near 50 ppb). The improvement between HIPPO and ATom is dramatic (Fig. 10). This is
2 partly due to the longer optical path length in the Model 211, as well as other instrumental improvements,
3 but the addition of the Nafion moisture exchangers makes a substantial difference as the aircraft transitions
4 from wet to dry air masses. It should be noted that the NOAA CSL instruments being compared to here have
5 completely different designs – Classic Ozone is a UV photometer like the 2B, while in ATom, ozone was
6 detected by chemiluminescence, though it is fundamentally calibrated using an optical measurement. Both of
7 these instruments have a precision in the troposphere of about ±0.5 ppb. The larger deviations occasionally
8 observed in the ATom data are mostly due to timing mismatches during flight segments with sharp gradients
9 in ozone, along with occasional outliers from all instruments (see Fig. A5). The older Model 205 was also
10 flown during ATom as a backup and for comparison with the Model 211; the Model 205 showed some of the
11 same deviations between wet and dry air as in HIPPO, while the Model 211 with Nafion moisture exchangers
12 tracked the CSD instrument closely. For many applications, such as climatologies, chemical modeling, and
13 transport studies in the troposphere, the precision of the Model 211 (±0.5 ppb at sea level) as flown during
14 ATom is more than adequate, given the good overall agreement with the chemiluminescence instrument. In
15 the stratospheric parts of the ATom flights, the Model 211 instrument had precision of about ±1% and
16 agreement within 2% (not shown).
17

18

Plot legend:
HIPPO 4
UCATS = a + b*CSL
a = 4.12 ± 0.07
b = 0.992 ± 0.0004
— Linear fit
— 1:1 line

X-axis: CSL Ozone (ppb)
Y-axis: UCATS Ozone (ppb)
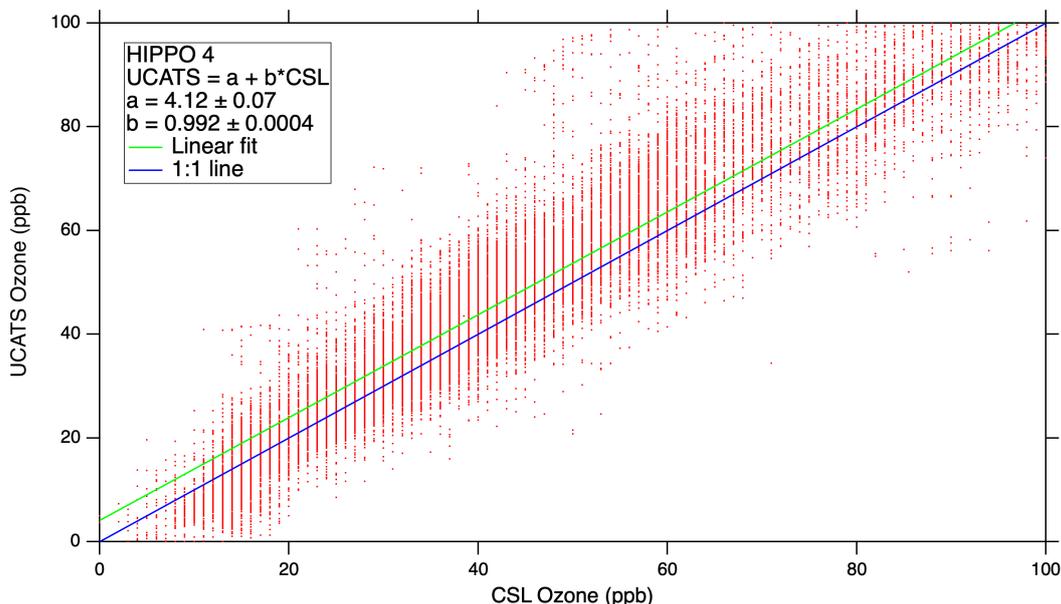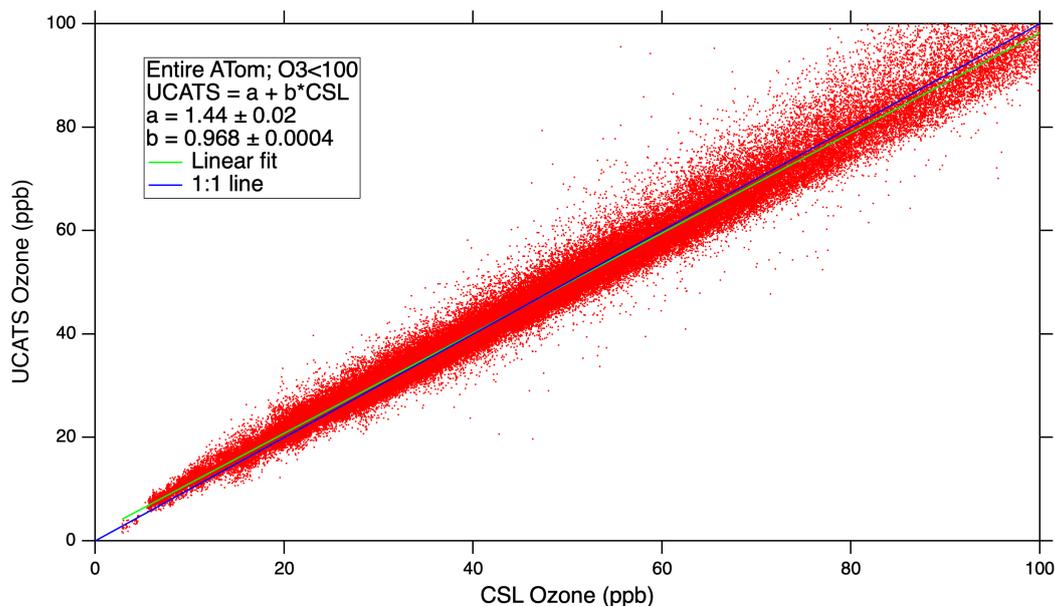
Figure 10: Scatter plots of UCATS ozone (2B Model 205) vs. CSL "Classic" ozone (top) and UCATS ozone (2B Model 211) vs. CSL chemiluminescence ozone (bottom) from tropospheric observations.

4.4 Water vapor

The original MayComm TDL instrument was used in UCATS from 2006 to the first ATom deployment in July-August 2016. Its uncertainty was the sum of 5% + 1 ppm, based on laboratory calibrations with gravimetrically-prepared standards and frost point hygrometers. The ±1 ppm precision limit made stratospheric measurements above ~16 km (where water vapor is typically 2-8 ppm) somewhat qualitative compared to the troposphere and lower stratosphere (H_2O > 10 ppm). In addition, there was a temperature effect on the electronics of the long-path channel (for low water vapor) such that the sensitivity dropped with increasing temperature inside UCATS, up to 30% in extreme cases. This was addressed by adding a Peltier cooling circuit to the TDL electronics box during HIPPO, which kept it at 25 °C (except on occasional cold or very warm takeoffs), and also by calibrating and correcting for the temperature effect.

For ATom (starting with deployment 2, January-February 2017), we integrated a new, larger TDL instrument from Port City Instruments, the successor to MayComm. The longer wavelength (2.574 μm vs. 1.37 μm) utilizes stronger absorption lines for a precision of ±0.1 ppm or better in the stratosphere; it can also measure up to 50000 ppm water vapor, higher than the maximum in the tropical MBL. Similar to the previous instrument, the large dynamic range was achieved by using two optical paths in the cell, strong and weak absorption lines, and different measurement techniques as described in Sect. 3. The data were found to have minimal or at least much less sensitivity to instrument temperature compared to the earlier version. For calibrations up to 200 ppm, we used ultra-pure air and gravimetrically prepared standards [Brewer et al., 2020]. We also calibrated the instrument over the full range of water vapor mixing ratios and pressures found in the troposphere and lower stratosphere (near 0 to ~30000 ppm and ~100-1000 mbar) with a bubbler and a frost point hygrometer (MBW, model 373LX). Air from the bubbler (or the standards) was passed through the TDL cell and then to the MBW, and also to both instruments in parallel. Illustrative plots and in-flight comparisons for both instruments are shown in Fig. 11. Calibrations of the TDL are ongoing, as disagreements with the DLH instrument were observed in ATom, particularly at very high water vapor mixing ratios, >20000 ppm, where the TDL data seem to be anomalously high (not shown).
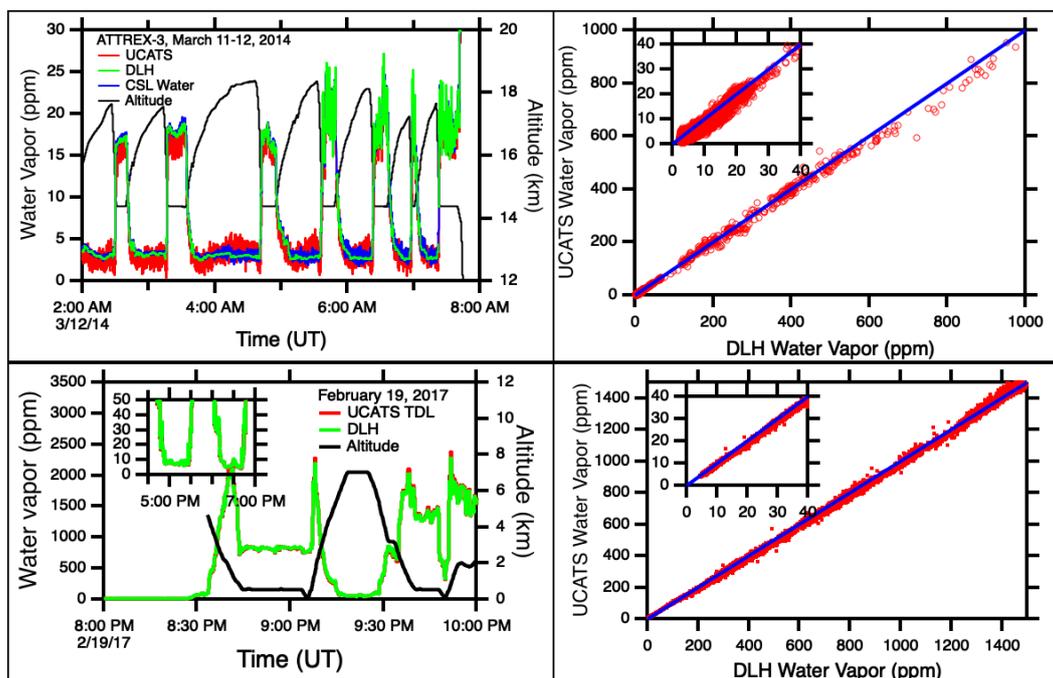
Figure 11: (top) Time series and scatter plots for UCATS TDL water, DLH, and NOAA Water (CSL) during ATTREX. The blue lines in the right hand plots are the 1:1 line for UCATS and DLH for the same flights as on the left. (bottom) Time series of the new UCATS TDL hygrometer and DLH, showing the improved precision at low water vapor mixing ratios. The right hand panel shows the good general agreement between UCATS and DLH over the low and middle range of mixing ratios for the same flight.

5 Summary and future plans

The UCATS instrument has successfully provided trace gas measurements on different types of aircraft for atmospheric science missions with diverse sets of objectives. After demonstration projects focused on the stratosphere, it was used for studies of stratosphere-troposphere exchange and atmospheric transport (START-08 and HIPPO), entry of air into the tropical stratosphere and TTL composition (ATTREX), and tropospheric chemistry (ATom). Over the course of these projects, UCATS evolved from a stratospheric instrument for small UAS payloads to an important contributor on multi-instrument campaigns and geographically extensive tropospheric missions. Challenges encountered and met included the effects of wet air on ozone and GC measurements, a range of instrument environments including pressurized and unpressurized locations with large differences in temperature (-20 °C on the Global Hawk to sometimes in excess of 30 °C on tropospheric missions), limitations on available space, as well as the requirements of each component in UCATS. Table A1 summarizes the quality of the data over several missions, reflecting improvements in stability for measurements of N_2O and SF_6 with comparable data quality, and improvements in precision and accuracy for ozone. Data from UCATS have been used to constrain the interhemispheric difference in OH radical concentrations [Patra et al., 2014] and quantify tropospheric age of air and transport using SF_6 [Waugh et al., 2013]. Studies have also been performed with UCATS data to probe the composition and structure of the TTL, including halogen chemistry [Jensen et al., 2017; Werner et al., 2017; Navarro et al., 2017], and hydroxyl radical reactivity in the remote troposphere [Thames et al., 2020].

At present, UCATS continues to evolve and is now being upgraded and repackaged for the NASA Dynamics and Chemistry of the Summer Stratosphere (DCOTSS) mission. The initial impetus for this change came from

1 the fact that the UCATS enclosure, extended to accommodate the new ozone and water instruments for ATom,
2 no longer fits in the vertical space available in the upper Q-Bay of the ER-2 aircraft, which will be used for
3 DCOTSS. Since the focus of DCOTSS is on stratospheric ozone and halogen chemistry, the GC channels are
4 being configured to measure N_2O, SF_6, and CFCs (as initially flown on Altair in 2005), and a third GC channel is
5 being added to measure shorter-lived chlorocarbons including chloroform ($CHCl_3$), carbon tetrachloride
6 (CCl_4), and trichloroethylene (C_2HCl_3). These changes will allow us to measure much of the organic chlorine
7 budget including the major long-lived organic chlorine compounds, and a few of the more short-lived ones.
8 The repackaged UCATS also has a cleaner and more rational layout, with modular and removeable GC
9 channels, ozone, and water instruments, and more modern electronics, flow controllers, and pressure
10 controllers. Test and science flights on the NASA ER-2 aircraft are now planned for 2021.

11
12 **Author contribution**
13
14 EJH maintained and operated the UCATS instrument since May 2009, analyzed the data presented here, and
15 wrote the manuscript, FLM designed and built UCATS, operated it on several missions, and worked closely
16 with it throughout, DFH operated UCATS on its first UAS missions and helped to prepare this manuscript, GS
17 Dutton, BDH, JDN, SAM, LPW, AM, and JWE assisted with laboratory work and field missions, JWE is the
18 principle investigator for UCATS for all NASA and NOAA missions, BRM, SAM, EGH, AFJ, AWR, TDT, LAW, CRT,
19 JP, IB, TBR, BCD, JVP, SCW, EK, GS Diskin, and TPB provided data and helped with other aspects of the field
20 missions. All the coauthors provided extensive comments and information for this manuscript.

21
22 **Competing interests**
23
24 The authors declare that they have no conflict of interest.

25
26 **Acknowledgements**
27

38
39 **Data availability**
40
41 HIPPO data are publicly available at https://www.eol.ucar.edu/field_projects/hippo; GloPac and ATTREX
42 data are available at https://espoarchive.nasa.gov/archive/browse/glopac and /attrex, and ATom data are
43 available at https://daac.ornl.gov/ATOM/campaign/.

44
45 **References**
46

47 Anderson, D. C., et al.: A pervasive role for biomass burning in tropical high ozone/low water structures,
48 Nature Commun., 7, doi:10.1038/ncomms10267, 2016.
49
50 Bourgeois, I., et al.: Global-scale distribution of ozone in the remote troposphere from ATom and HIPPO
51 airborne field missions, Atmos. Chem. Phys., 20, 10611-10635, doi:10.5194/acp-20-10611-2020, 2020.
52
53 Brewer, P. J., Gieseking, B., Ferracci, V. F., Ward, M., Carroll, P., Bell, S., and Hall, B.: International pilot study
54 CCQM-P193: 10 μmol/mol water vapour in nitrogen, Metrologia, 57, doi:10.1088/0026-1394/57/1A/08015,
55 2020.

1
2 Diskin, G. S., Podolske, J. R., Sachse, G. W., and Slate, T. A.: Open-path airborne tunable diode laser hygrometer,
3 Diode Lasers and Applications in Atmospheric Sensing, 4817, International Society for Optics and Photonics,
4 doi:10.1117/12.453736, 2002.
5
6 Douglass, A. R., Newman, P. A., and Solomon, S.: The Antarctic ozone hole: An update, Phys. Today, 67, 42–48,
7 doi:10.1063/PT.3.2449, 2014.
8
9 Elkins, J. W., et al.: Airborne gas chromatograph for *in situ* measurements of long-lived species in the upper
10 troposphere and lower stratosphere, Geophys. Res. Lett., 23, 347-350, doi:10.1029/96GL00244, 1996.
11
12 Fahey, D. W., et al.: Altair Unmanned Aircraft System Achieves Demonstration Goals, EOS Trans. AGU, 87, 197-
13 201, doi:10.1029/2006EO200002, 2006.
14
15 Farman, J. C., Gardiner, B. G., and Shanklin, J. D.: Large losses of total ozone in Antarctica reveal seasonal
16 ClO_x/NO_x interaction, Nature, 315, 207–210, doi:10.1038/315207a0, 1985.
17
18 Fueglistaler, S., Dessler, A. E., Dunkerton, T. J., Folkins, I., Fu, Q., and Mote, P. W.: Tropical Tropopause Layer,
19 Rev. Geophys., 47, RG1004, doi:10.1029/2008RG000267, 2009.
20
21 Gao, R. S., Ballard, J., Watts, L. A., Thornberry, T. D., Ciciora, S. J., McLaughlin, R. J., and Fahey, D. W.: A compact,
22 fast UV photometer for measurement of ozone from research aircraft, Atmos. Meas. Tech., 5, 2201–2210,
23 doi:10.5194/amt-5-2201-2012, 2012.
24
25 Hall, B. D., Dutton, G. S., Mondeel, D. J., Nance, J. D., Rigby, M., Butler, J. H., Moore, F. L., Hurst, D. F., and Elkins, J.
26 W.: Improving measurements of SF_6 for the study of atmospheric transport and emissions, Atmos. Meas.
27 Tech., 4, 2441-2451, doi: 10.5194/amt-4-2441-2011, 2011.
28
29 Hinkley, E., Ambrosia, V., Toscano, W. M., and Zajkowski, T.: NASA Partners with Forest Service on Fire
30 Mission, Tech. Innovation, 15, 28-30, 2009.
31
32 Jensen, E. J., et al.: The NASA Airborne Tropical TRopopause EXperiment (ATTREX), SPARC Newsletter, 41, 15,
33 2013.
34
35 Jensen, E. J., et al.: Physical processes controlling the spatial distributions of relative humidity in the tropical
36 tropopause layer over the Pacific, J. Geophys. Res., 122, 6094, doi:10.1002/2017JD026632, 2017.
37
38 Komhyr, W. D., Barnes, R. A., Brothers, G. B., Lathrop, J. A., and Opperman, D. P.: Electrochemical concentration
39 cell ozonesonde performance evaluation during STOIC 1989, J. Geophys. Res., 100, 9231–9244,
40 doi:10.1029/94JD02175, 1995.
41
42 Moore, F. L., et al.: Balloonborne *in situ* gas chromatograph for measurements in the troposphere and
43 stratosphere, J. Geophys. Res., 108, 8330, doi:10.1029/2001JD000891, 2003.
44
45 Navarro, M. A., Saiz-Lopez, A., Cuevas, C. A., Fernandez, R. P., Atlas, E., Rodriguez-Lloveras, X., Kinnison, D.,
46 Lamarque, J.-F., Tilmes, S., Thornberry, T., Rollins, A., Elkins, J. W., Hintsa, E. J., and Moore, F. L.: Modeling the
47 inorganic bromine partitioning in the tropical tropopause layer over the eastern and western Pacific Ocean,
48 Atmos. Chem. Phys., 17, 9917–9930, doi:10.5194/acp-17-9917-2017, 2017.
49
50 Pan, L. L., Bowman, K. P., Atlas, E. L., Wofsy, S. C., Zhang, F., Bresch, J. F., Ridley, B. A., Pittman, J. V., Homeyer, C.
51 R., Romashkin, P., and Cooper, W. A.: The Stratosphere-Troposphere Analyses of Regional Transport 2008
52 (START08) Experiment, Bull. Amer. Meteor. Soc., 91, 327-342, 2010.
53
54 Pan, L. L., et al.: Bimodal distribution of free tropospheric ozone over the tropical western Pacific revealed by
55 airborne observations, Geophys. Res. Lett., 42, doi:10.1002/2015GL065562, 2015.

Atmospheric
Measurement
Techniques
Discussions

Pan, L. L., et al.: The Convective Transport of Active Species in the Tropics (CONTRAST) Experiment, Bull. Am. Met. Soc., 98, 106-128, doi:10.1175/BAMS-D-14-00272.1, 2017.

Patra, P. K., et al.: Observational evidence for interhemispheric hydroxyl-radical parity, Nature, 513, 219-223, doi.org/10.1038/nature13721, 2014.

Plumb, R. A. and Ko, M. K. W.: Interrelationships between mixing ratios of long-lived stratospheric constituents, J. Geophys. Res., 97, 10145-10156, doi: 10.1029/92JD00450, 1992.

Podolske, J. R., Sachse, G. W., and Diskin, G. S.: Calibration and data retrieval algorithms for the NASA Langley/Ames Diode Laser Hygrometer for the NASA Transport and Chemical Evolution Over the Pacific (TRACE-P) mission, J. Geophys. Res., 108, 8792, doi:10.1029/2002JD003156, 2003.

Proffitt, M. H. and McLaughlin, R. J.: Fast-response dual-beam UV-absorption ozone photometer suitable for use on stratospheric balloons, Rev. Sci. Instrum., 54, 1719–1728, doi:10.1063/1.1137316, 1983.

Ridley, B. A., Grahek, F. E., and Walega, J. G.: A Small High-Sensitivity, Medium-Response Ozone Detector Suitable for Measurements from Light Aircraft, J. Atmos. Oceanic Technol., 9, 142–148, doi:10.1175/1520-0426(1992)009<0142:ASHSMR>2.0.CO;2, 1992.

Romashkin, P. A., Hurst, D. F., Elkins, J. W., Dutton, G. S., Fahey, D. W., Dunn, R. E., Moore, F. L., Myers, R. C., and Hall, B. D.: *In situ* measurements of long-lived trace gases in the lower stratosphere by gas chromatography, J. Atm. Ocean. Tech., 18, 1195-1204, doi:10.1175/1520-0426(2001)018<1195:ISMOLL>2.0.CO;2, 2001.

Santoni, G. W., et al.: Evaluation of the airborne quantum cascade laser spectrometer (QCLS) measurements of the carbon and greenhouse gas suite – CO_2, CH_4, N_2O, and CO – during the CalNex and HIPPO campaigns, Atmos. Meas. Tech., 7, 1509–1526, doi:10.5194/amt-7-1509-2014, 2014.

Schauffler, S. M., Atlas, E. L., Blake, D. R., Flocke, F., Lueb, R. A., Lee-Taylor, J. M., Stroud, V., and Travnicek, W.: Distributions of brominated organic compounds in the troposphere and lower stratosphere, J. Geophys. Res., 104, 21,513-21,535, doi:10.1029/1999JD900197, 1999.

Scott, S. G., Bui, T. P., Chan, K. R., and Bowen, S. W.: The Meteorological Measurement System on the NASA ER-2 Aircraft, J. Atmos. Oceanic Technol., 7, 525–540, doi:10.1175/1520-0426(1990)007<0525:TMMSOT>2.0.CO;2, 1990.

Sweeney, C., Karion, A., Wolter, S., Newberger, T., Guenther, D., Higgs, J. A., Andrews, A. E., Lang, P. M., Neff, D., Dlugokencky, E., Miller, J. B., Montzka, S. A., Miller, B. R., Masarie, K. A., Biraud, S. C., Novelli, P. C., Crotwell, M., Crotwell, A. M., Thoning, K., and Tans, P. P.: Seasonal climatology of CO2 across North America from aircraft measurements in the NOAA/ESRL Global Greenhouse Gas Reference Network, J. Geophys. Res., 120, 5155–5190, doi:10.1002/2014JD022591, 2015.

Thames, A. B., et al.: Missing OH reactivity in the global marine boundary layer, Atmos. Chem. Phys., 20, 4013–4029, doi:10.5194/acp-20-4013-2020, 2020.

Waugh, D. W., Crotwell, A. M., Dlugokencky, E. J., Dutton, G. S., Elkins, J. W., Hall, B. D., Hintsa, E. J., Hurst, D. F., Montzka, S. A., Mondeel, D. J., Moore, F. L., Nance, J. D., Ray, E. A., Steenrod, S. D., Strahan, S. E., and Sweeney, C.: Tropospheric SF6: Age of air from the Northern Hemisphere midlatitude surface, J. Geophys. Res., 118, 11,429–11,441, doi:10.1002/jgrd.50848, 2013.

Werner, B., et al.: Probing the subtropical lowermost stratosphere and the tropical upper troposphere and tropopause layer for inorganic bromine, Atmos. Chem. Phys., 17, 1161–1186, doi:10.5194/acp-17-1161-2017, 2017.

Atmospheric
Measurement
Techniques
Discussions

Wilson, K. L. and Birks, J. W.: Mechanism and Elimination of a Water Vapor Interference in the Measurement of Ozone by UV Absorbance, Environ. Sci. Technol., 40, 6361-6367, doi:10.1021/es052590c, 2006.

Wofsy, S. C.: HIAPER Pole-to-Pole Observations (HIPPO): fine-grained, global-scale measurements of climatically important atmospheric gases and aerosols, Phil. Trans. R. Soc. A, 369, 2073–2086, doi:10.1098/rsta.2010.0313, 2011.

Appendix A to:

UAS Chromatograph for Atmospheric Trace Species (UCATS) – a versatile instrument for trace gas measurements on airborne platforms

Eric J. Hintsa et al.

Table of contents:

Further details about the UCATS instrument and results from different campaigns are collected here. They include schematics of the ozone and water components, additional data and comparison figures, and details about precision and agreement with other measurements.

1 Ozone and water instrument schematics
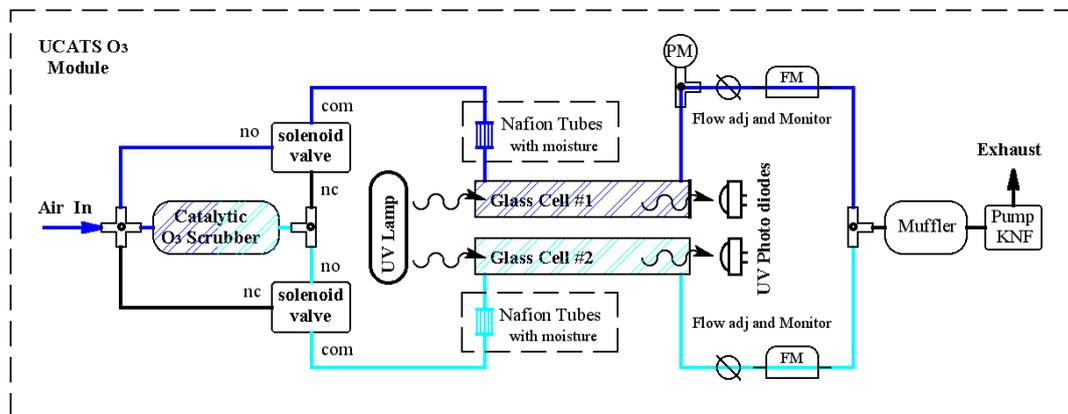
Figure A1a: For all 2B ozone sensors in UCATS, ambient air is split into two paths, one of which is catalytically scrubbed of ozone with MnO_2-coated screens, then alternately sent to the two cells on a 2-second cycle ("no" = normally open, "nc" = normally closed, "com" = common). The other cell is flushed with ambient air, and a measurement is made every 2 seconds. Data are averaged to 10 seconds or output at the original 2-second rate. For the Model 211, we humidified the air flow prior to entering the cells with Nafion moisture exchangers. Cell

1   pressure is measured at the outlet of one of the cells ("PM"), and on the Model 211, flows are measured ("FM")
2   and can be manually adjusted upstream of the pump. A small settling volume can also be used upstream of the
3   pump to minimize pressure fluctuations.
4
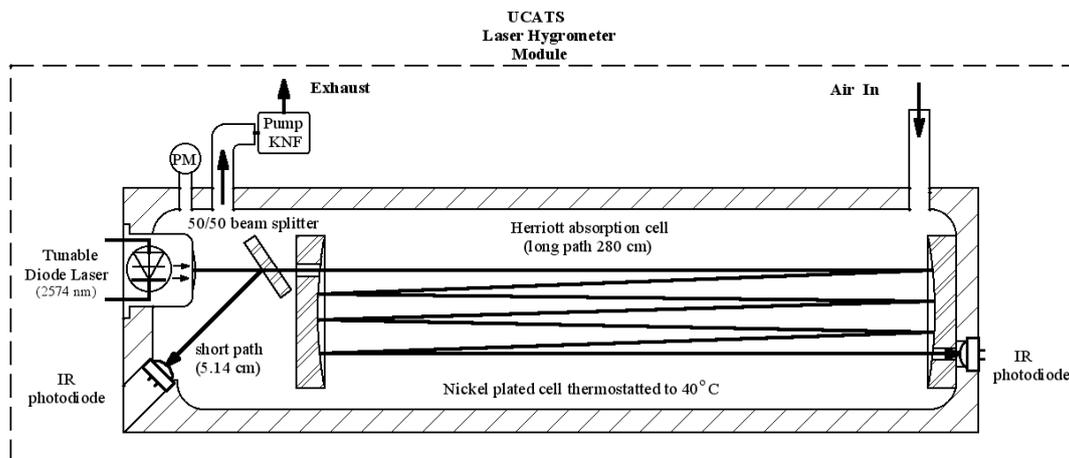
5
6
7   **Figure A1b: The absorption cell for the Port City TDL hygrometer has the diode laser at one end, with a partially**
8   **reflecting mirror located approximately 2.5 cm from the laser and radiation reflected back to a sealed**
9   **photodiode for the short path (high water vapor) measurement. The remainder of the beam is directed by**
10 **mirrors through a Herriot cell arrangement to a diode opposite the laser for the long-path measurement. Air**
11 **flows into the cell through the port farther away from the laser and pressure is measured right at the outlet of the**
12 **cell to avoid trapped air volumes and to promote smooth flow through the cell. The electronics are in a separate**
13 **box (not shown). In the earlier Maycomm version, the laser was together with the electronics and reached the**
14 **cell through fiber optic cables, but the cell geometry was similar overall, except that the pressure sensor was in**
15 **the middle of the cell, which could lead to issues with trapped air and delays in the cell drying out after**
16 **transitions between wet and dry air masses.**
17

1   **2 Tropical N$_2$O and SF$_6$ data**
2

3
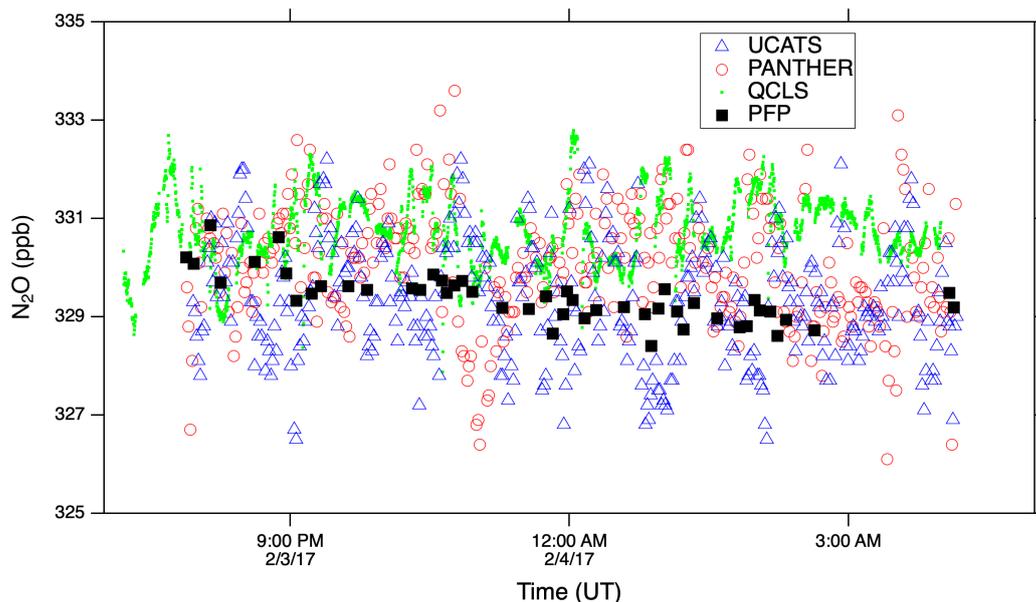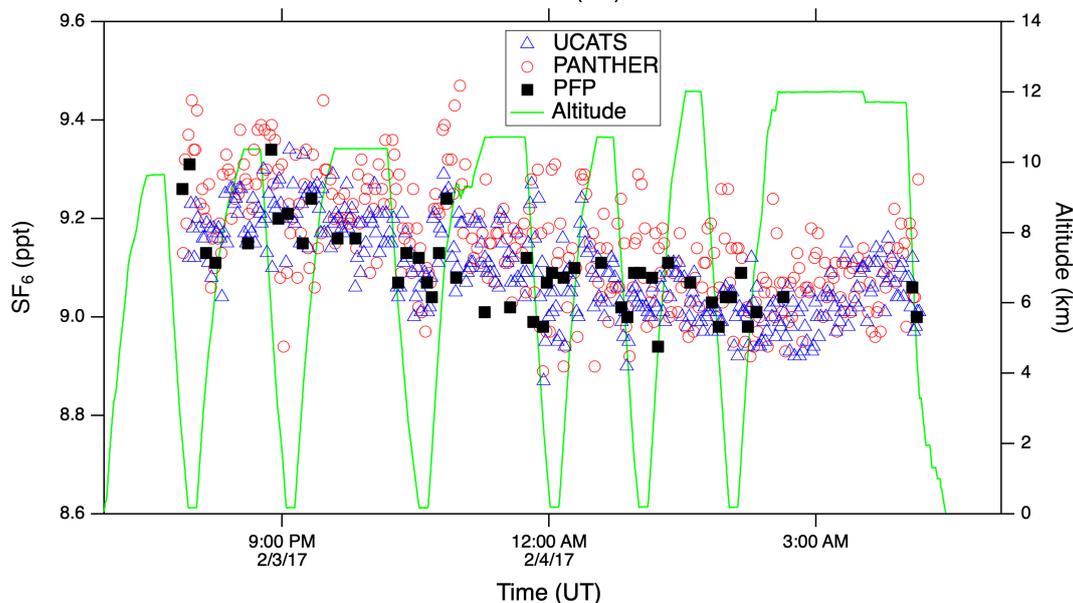
4
5   **Figure A2: N$_2$O (top) and SF$_6$ (bottom) time series plots from the February 3, 2017 ATom-2 flight from Kona, HI to**
6   **Fiji through the tropics. The precision of the *in situ* instruments was near 1 ppb N$_2$O and 0.05 ppt SF$_6$.**
7   **Throughout this flight the DC-8 remained in the troposphere. The weak vertical gradients in these long-lived**
8   **tracers (compare to Fig. 5 at high latitudes) allows the latitudinal gradient to be easily discerned (lower values in**
9   **the Southern Hemisphere), particularly for SF$_6$. Flights through very humid air tested the ability of UCATS to**
10 **maintain stable chromatography and good precision.**
11

Atmospheric
Measurement
Techniques
Discussions
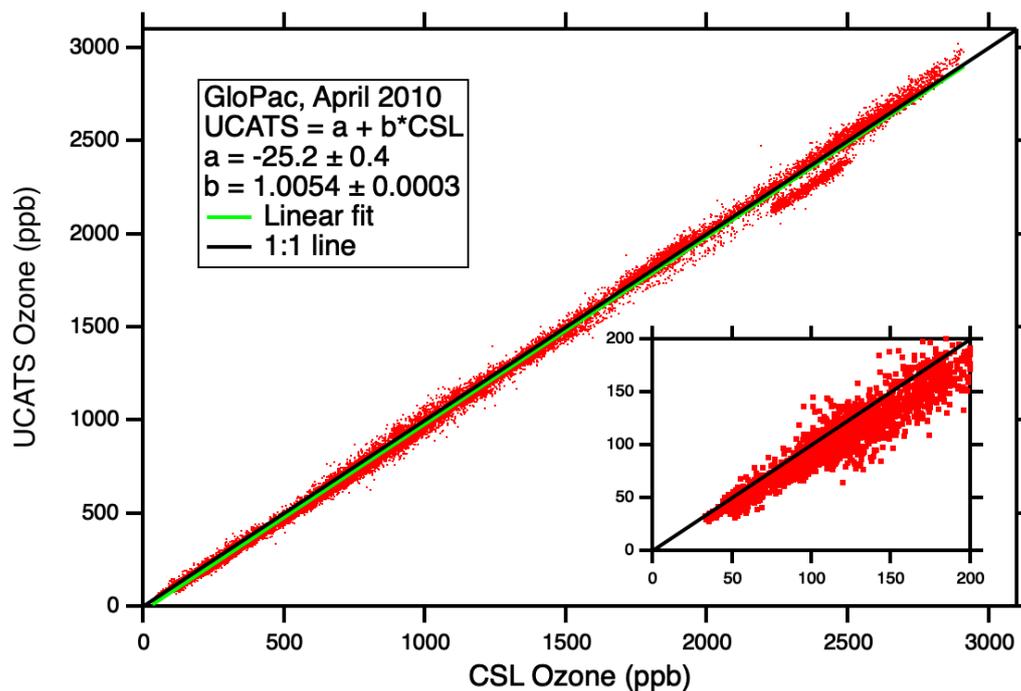
1   **3 GloPac ozone**
2

3
4
5   **Figure A3: Comparison of UCATS (Model 205) ozone against NOAA CSL Classic Ozone for the entire set of GloPac**
6   **flights. With its long range and duration, including a 28-hour flight on April 23, 2010, the Global Hawk sampled a**
7   **wide range of air masses from the tropics to the North Pole, including a polar vortex fragment. It encountered**
8   **very high ozone values considering its maximum altitude is just over 19 km; this was possible during and after**
9   **the season of strong descent near the northern hemisphere polar vortex. Almost all the data shown here were**
10   **obtained in the stratosphere; no attempt was made to exclude data from the troposphere on ascents, descents,**
11   **and vertical profiles in the tropics. The linear fit line is always below the 1:1 line in this plot, but UCATS data**
12   **were actually about 0-1% higher than Classic Ozone at the highest values, and UCATS data were about 4.5 ppb**
13   **lower at the lowest ozone (30-40 ppb, see inset); the linear fit parameters do not quite capture the complete**
14   **range of the observations.**
15

1   **4 ATTREX ozone consistency between different platforms**
2
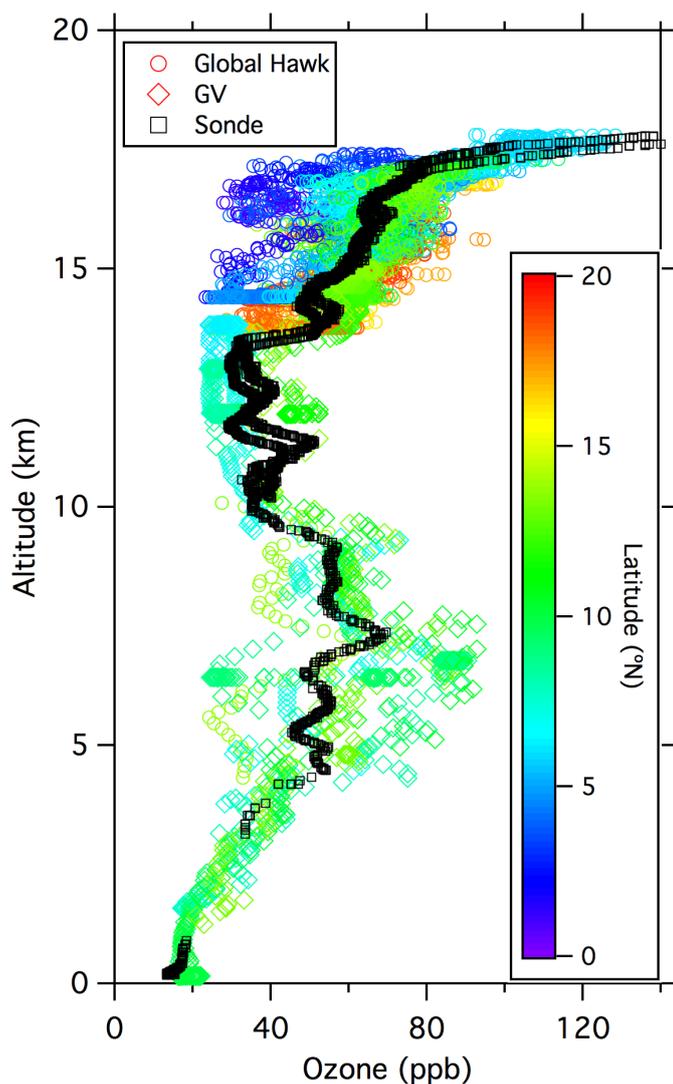
3
4
5   **Figure A4: Combined ozone data from the Global Hawk (UCATS) on February 12-13 (circles; mainly above 12 km),**
6   **the GV (NCAR) on February 12 (diamonds; 0-14 km), and the ozonesonde (NOAA GML) launch on February 13**
7   **(black squares). The aircraft data are color-coded by latitude; the sonde data (both ascent and descent) are all**
8   **from near Guam (13.5°N) and would appear light green if color-coded. These were not coincident measurements,**
9   **as the two aircraft sampled different air masses and the sonde was launched one day later than the GV flight, but**
10   **the two-day comparison shows consistency between the various measurements and many of the typical features**
11   **encountered in February 2014 over the western tropical Pacific. Ozone was low at the surface (~20 ppb), with**
12   **large variability in the mid-troposphere (Pan et al., 2015, Anderson et al., 2016) caused by frequent encounters**
13   **with filaments of high ozone air over a much lower background. A second minimum is visible in the upper**
14   **troposphere up to the base of the TTL. In the TTL, ozone gradually increased with increasing altitude, with large-**
15   **scale variations related to latitude and long-range transport, then increased much more sharply near the top of**
16   **the TTL (~17.5 km or 380 K), as air with greater stratospheric character was sampled.**

1 **5 Ozone gradients and precision**
2

3
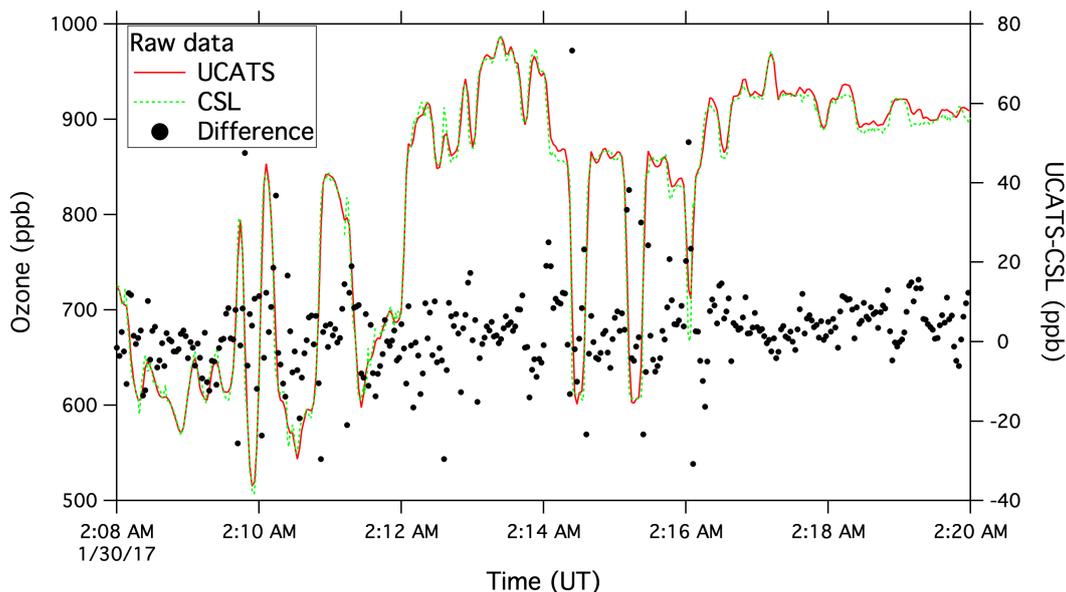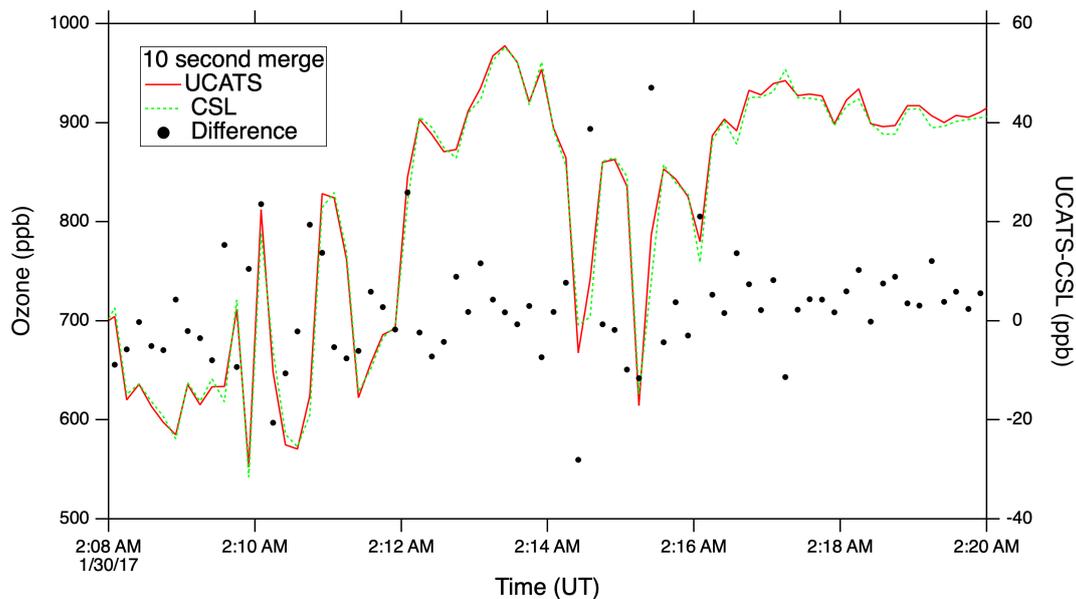
4
5
6 **Figure A5: Archived UCATS and CSL ozone data for the ATom flight of January 29, 2017, from Palmdale, CA to**
7 **Anchorage, AK (top). The black circles indicate the difference between the two instruments, with 1-second CSL**
8 **data interpolated to match the sampling times of the 2-second UCATS data. Other than adjustments for timing, no**
9 **corrections were made to either data set. The visual agreement for the time series is impressive, with both**
10 **instruments capturing the atmospheric variability, but nonetheless the black circles indicate differences over 40**
11 **ppb in places. As noted in the main text, this is due to slight offsets in timing, and also from the fact that the 2B**
12 **instrument has a short "dead time" when flows switch between cells, whereas the CSL data are essentially**

1   continuous, and reported at 1 Hz for ease of use and to achieve good signal-to-noise. Where ozone is varying
2   rapidly, such as this level flight leg at 11.3 km, or ascents and descents, these two effects lead to many of the
3   "outliers" in comparison plots (such as the ATom panel in Fig. 10). The lower plot shows the same data, but from
4   the 10-second merge file commonly used for analyses. Some of the fine structure in the raw data is washed out,
5   but there are still differences of up to 5%, even though the two data sets appear to match almost perfectly. As an
6   example of the precision possible with the UCATS instrument, we analyzed a segment with much less variability
7   near the ocean surface on May 29, 2019 (not shown). Here, ozone was low and nearly constant for about 6
8   minutes, the mean difference between data from the two instruments was 0.4 ppb, and the standard deviation of
9   the difference was 0.5 ppb for the 10-second merge and 0.7 ppb for 2-second data.

1
2 **Table A1 Precision of UCATS measurements and agreement with other instruments and ground sites.**
3

Mission	Year	Molecule	Precision	Agreement with onboard instruments	Agreement with surface network
HIPPO	2009-11	N2O	1.5 ppb	1 ppb	<1 ppb
		SF6	0.05 ppt	0.05 ppt	0.03 ppt
		CH4	15 ppb	10 ppb	15 ppb
		H2	5 ppb	5 ppb	—
		O3	9 ppb	3 ppb	—
		H2O	1 ppm[a]	5%	—
GloPac/	2010	N2O	1 ppb	—	—
ATTREX	2011-15	SF6	0.04 ppt	—	—
		CH4	7 ppb	<5 ppb	—
		H2	5 ppb	—	—
		O3	5-10 ppb[b]	<1 ppb[b]	—
		H2O	1 ppm	5%	—
ATom	2016-18	N2O	1 ppb	1.5 ppb	0.8 ppb
		SF6	0.05 ppt	<0.05 ppt	0.04 ppt
		CH4	15 ppb	<5 ppb	10 ppb
		H2	5 ppb	5 ppb	—
		O3	2-3 ppb	<1 ppb	—
		H2O	0.1 ppm	in process	—

4
5 **Table A1: Precision of UCATS measurements for selected missions, level of agreement with other instruments on**
6 **the same platform, and comparison of lower tropospheric values of long-lived gases with the NOAA surface**
7 **network. The NOAA surface network of flask collection sites allows the airborne measurements to be tied to a**
8 **global system with calibration scales for all the gases measured by GC. The NOAA airborne instruments use**
9 **standards from the same laboratory as the surface network, as well as the same scales. CO is not included**
10 **because it was usually measured by other instruments, and has an artifact in the stratosphere at high ozone**
11 **levels. In the troposphere the precision for CO was typically 5-10 ppb. The main sink of H_2 is at the surface and it**
12 **has the most variability there, so we do not compare it with the surface network. Not all deployments and**
13 **measurements achieved the same level of precision as shown here. This table applies to HIPPO 1 for long-lived**
14 **gases, GloPac and ATTREX-2 and 3 for N_2O and SF_6, and ATom-2, 3, and 4 for all species measured by UCATS.**
15
16 **[a]Precision for water vapor is best expressed as a percentage in the troposphere (high water vapor) and an**
17 **absolute number in the stratosphere (low water). The precision here is given for the lowest water vapor values**
18 **in the stratosphere, 1 ppm for the original MayComm instrument and 0.1 ppm for the newer Port City instrument.**
19 **The precision in the troposphere was always 5% or better. Calibration and comparison of the Port City**
20 **instrument are still ongoing.**
21
22 **[b]The precision and agreement for ozone are best expressed in ppb at low mixing ratios, and as a percentage at**
23 **high mixing ratios. For example, in ATTREX and GloPac, where ozone ranged from less than 20 ppb to over 2000**
24 **ppb, the average agreement with the CSL instrument was better than 1 ppb for ozone < 200 ppb, with a precision**
25 **better than 10 ppb, and for ozone > 500 ppb, the average agreement was better than 1% with a precision of 2-3%.**
26 **Values for ATom are for tropospheric data (O_3<100 ppb), since the focus of ATom was on tropospheric chemistry.**
27